

University of New Hampshire

University of New Hampshire Scholars' Repository

Faculty Publications

8-6-2022

Microtopography Matters: Belowground CH₄ Cycling Regulated by Differing Microbial Processes in Peatland Hummocks and Lawns

Clarice R. Perryman

University of New Hampshire, Durham

Carmody K. McCalley

Rochester Institute of Technology

Jessica G. Ernakovich

University of New Hampshire, Durham

Louis J. Lamit

Syracuse University

Joanne H. Shorter

Aerodyne Research Inc.

Follow this and additional works at: https://scholars.unh.edu/faculty_pubs



next page for additional authors
Part of the [Biogeochemistry Commons](#)

Comments

This is a preprint of an author's manuscript published by Wiley in JGR: Biogeosciences in 2022, the Version of Record is available online: <https://dx.doi.org/10.1029/2022JG006948>

Recommended Citation

Perryman, C. R., McCalley, C. K., Ernakovich, J. G., Lamit, L. J., Shorter, J. H., Lilleskov, E., & Varner, R. K. (2022). Microtopography matters: Belowground CH₄ cycling regulated by differing microbial processes in peatland hummocks and lawns. *Journal of Geophysical Research: Biogeosciences*, 127, e2022JG006948. <https://doi.org/10.1029/2022JG006948>

This Article is brought to you for free and open access by University of New Hampshire Scholars' Repository. It has been accepted for inclusion in Faculty Publications by an authorized administrator of University of New Hampshire Scholars' Repository. For more information, please contact Scholarly.Communication@unh.edu.

Authors

Clarice R. Perryman, Carmody K. McCalley, Jessica G. Ernakovich, Louis J. Lamit, Joanne H. Shorter, Erik Lilleskov, and Ruth K. Varner

Microtopography matters: Belowground CH₄ cycling regulated by differing microbial processes in peatland hummocks and lawns

Clarice R. Perryman^{1,2*}, Carmody K. McCalley³, Jessica G. Ernakovich⁴, Louis J. Lamit⁵, Joanne H. Shorter⁶, Erik Lilleskov⁷, Ruth K. Varner^{1,2#}

¹Department of Earth Sciences, University of New Hampshire, Durham, NH, USA.

²Institute for the Study of Earth, Oceans, and Space, University of New Hampshire, Durham, NH, USA.

³Thomas H. Gosnell School of Life Sciences, Rochester Institute of Technology, Rochester, NY, USA.

⁴Department of Natural Resources and the Environment, University of New Hampshire, Durham, NH, USA. ORCID: 0000-0002-4493-2489

⁵ Department of Biology, Syracuse University, Syracuse, NY, USA, and Department of Environmental and Forest Biology, State University of New York College of Environmental Science and Forestry, Syracuse, New York, USA.

⁶Aerodyne Research Inc., Billerica, MA, USA.

⁷USDA Forest Service, Northern Research Station, Houghton, MI, USA. ORCID: 0000-0002-9208-1631

* ORCID: 0000-0002-5086-6684

ORCID: 0000-0002-3571-6629

Corresponding author: Clarice R. Perryman (clarice.perryman@unh.edu)

Key Points:

- Surface porewater $\delta^{13}\text{C-CH}_4$ and $\delta\text{D-CH}_3\text{D}$ values were more reflective of methanotrophy in hummocks and methanogenesis in lawns
- Community composition of methanogens and methanotrophs was influenced by redox conditions and water table level across microtopography
- Vegetation cover had limited influence on microbial community composition and porewater CH₄ concentration and stable isotope composition

This is the author manuscript accepted for publication and has undergone full peer review but has not been through the copyediting, typesetting, pagination and proofreading process, which may lead to differences between this version and the [Version of Record](#). Please cite this article as [doi: 10.1029/2022JG006948](https://doi.org/10.1029/2022JG006948).

This article is protected by copyright. All rights reserved.

Abstract

Water table depth and vegetation are key controls of methane (CH_4) emissions from peatlands. Microtopography integrates these factors into features called microforms. Microforms often differ in CH_4 emissions, but microform-dependent patterns of belowground CH_4 cycling remain less clearly resolved. To investigate the impact of microtopography on belowground CH_4 cycling, we characterized depth profiles of the community composition and activity of CH_4 -cycling microbes using 16S rRNA amplicon sequencing, incubations, and measurements of porewater CH_4 concentration and isotopic composition from hummocks and lawns at Sallie's Fen in NH, USA. Geochemical proxies of methanogenesis and methanotrophy indicated that microforms differ in dominant microbial CH_4 cycling processes. Hummocks, where water table depth is lower, had higher porewater redox potential (Eh) and higher porewater $\delta^{13}\text{C}\text{-CH}_4$ values in the upper 30 cm than lawns, where water table depth is closer to the peat surface. Porewater $\delta^{13}\text{C}\text{-CH}_4$ and $\delta\text{D}\text{-CH}_3\text{D}$ values were highest at the surface of hummocks where the ratio of methanotrophs to methanogens was also greatest. These results suggest that belowground CH_4 cycling in hummocks is more strongly regulated by methanotrophy, while in lawns methanogenesis is more dominant. We also investigated controls of porewater CH_4 chemistry. The ratio of the relative abundance of methanotrophs to methanogens was the strongest predictor of porewater CH_4 concentration and $\delta^{13}\text{C}\text{-CH}_4$, while vegetation composition had minimal influence. As microbial community composition was strongly influenced by redox conditions but not vegetation, we conclude that water table depth is a stronger control of belowground CH_4 cycling across microforms than vegetation.

Plain Language Summary

Northern peatlands are significant sources of the greenhouse gas methane (CH_4) to the atmosphere. Patterns of CH_4 emissions across peatlands often mirror patterns in water table level, vegetation cover, and elevation over small spatial scales as these factors influence microbial CH_4 production and consumption. We investigated microbial CH_4 production and consumption across areas in a northern peatland with varying water table depth and vegetation cover using measurements of belowground CH_4 chemistry and microbial DNA sequencing. We observed consistent signals in the belowground concentration and stable isotope composition of CH_4 , which can indicate where different microbial processes are occurring, that suggest slightly elevated areas with lower water table depth are hotspots for CH_4 consumption while CH_4 production is more prominent in areas that are lower and wetter. Overall, both CH_4 chemistry and microbial communities were more strongly influenced by changes in moisture than vegetation. These insights are important for understanding how climate change may impact CH_4 cycling, as CH_4 producing and consuming microbes respond differently to changes in temperature and moisture. Better understanding of the distribution of CH_4 production and consumption across the landscape may also help scale predictions of CH_4 emissions across larger areas for global modelling efforts.

1 Introduction

Given the disproportionate share of global soil carbon (C) stored in peatlands (Hugelius et al., 2020; Yu, 2012), factors that control the decomposition and release of peatland C are a pressing concern. Particular attention has been given to methane (CH_4) emissions from peatlands due to the large global warming potential of CH_4 (Etminan et al., 2016). Methane emissions from peatlands are affected by interannual and seasonal climate variability that regulate ambient air

and peat temperature and water table position (Bubier et al., 1995; Crill et al., 1988; Granberg et al., 2001; Olson et al., 2013), as well as vegetation community composition (Noyce et al., 2014). Water table depth and vegetation also impact the community composition and/or activity of methanogenic and methanotrophic microbes (Lamit et al., 2021; Siljanen et al., 2011; Urbanová & Bárta, 2020; Robroek et al., 2015) that regulate CH₄ emissions by mediating belowground CH₄ cycling (Freitag et al., 2010; Rey-Sanchez et al., 2019).

Changes in water table position and vegetation in peatlands often covary across the landscape with changes in land surface elevation, or microtopography. Across northern peatlands, CH₄ emissions generally increase along a landscape gradient from dry, raised hummocks with shrubby vegetation, to lawns with intermediate water table depth and more abundant sedges, to hollows which are seasonally to permanently inundated (Bubier et al., 1993; Frenzel and Karofeld, 2000; Kettunen et al., 2003). The variation in CH₄ emissions observed between microtopographic units, called microforms, is attributed to both the increase in the water table level, which promotes anaerobic methanogenesis and suppresses aerobic methanotrophy (Knorr et al., 2008; Yrjälä et al., 2011), and an increase in sedges (Greenup et al., 2000). Shifts in the abundance of sedges across peatland microforms are particularly relevant to CH₄ cycling as sedges have aerenchyma that allow gas exchange between aboveground shoots to roots tips below the water table. Variation in sedge abundance may substantially alter CH₄ cycling across microtopography given sedges' influence on gas transport (Noyce et al., 2014), methanogenic pathways and substrates (Hines et al., 2008; Saarnio et al., 2004), and methanotrophy (Popp et al., 2000; Strom et al., 2005).

Microform-dependent patterns of belowground CH₄ cycling and microbial communities remain less clearly resolved than patterns of CH₄ fluxes across microforms. Potential rates of CH₄ production are generally higher in more saturated lawns and hollows (Frenzel and Karofeld, 2000; Krohn et al., 2017; Zalman et al., 2018), but patterns in potential CH₄ oxidation are less clear (Sundh et al., 1994; van Winden, 2012). Furthermore, previous observations of the community composition of methanogens and methanotrophs across peatland microforms contradict, with some studies finding that microtopography strongly influences microbial community composition (Asemaninejad et al., 2019; Chroňáková et al., 2019), and others finding few differences between microforms (Deng et al., 2014; Juottonen et al., 2015; Kip et al., 2012; Martí et al., 2015). One way to resolve the inconsistencies observed in previous studies examining belowground CH₄ cycling across peatland microforms is to examine the isotopic composition of CH₄ in peat porewater. The isotopic composition of porewater CH₄ provides insight into dominant belowground microbial processes, as acetoclastic methanogenesis, hydrogenotrophic methanogenesis, and methanotrophy have characteristic effects on the C (¹²C vs. ¹³C) and hydrogen (¹H vs. ²H, or deuterium, D) isotope composition of CH₄ (Coleman et al., 1981; Chanton et al., 2005; Whitcar et al., 1986). There has been limited use of stable isotopes to characterize belowground CH₄ cycling across peatland microforms, and to date these observations only consider C isotopes. In consistently water-saturated peat (0.5 to 2 m below peat surface), porewater δ¹³C-CH₄ appears homogenous across hummocks, lawns, and hollows (Dorodnikov et al., 2013), but in the upper peat column porewater δ¹³C-CH₄ may help illuminate how zones of CH₄ production and oxidation vary depending on the location of the water table (Kato et al., 2013). As such, there is a need to further characterize patterns of porewater δ¹³C-CH₄ and δD-CH₃D across peatland microforms, especially in the upper portion of the peat

column where redox conditions have greater variability across microforms with differing water table depth.

In this study, we investigated belowground CH₄ cycling in hummocks and lawns of a northern temperate peatland in order to compare the potential rates and controls of CH₄ cycling between these microforms. We assessed the activity and community composition of methanogens and methanotrophs using laboratory incubations, porewater CH₄ concentration, δ¹³C-CH₄, and δD-CH₃D measurements, and 16S rRNA amplicon sequencing. We aimed to resolve the relationships between water table depth, vegetation, methanogen and methanotroph relative abundance, and porewater CH₄ concentration and isotopic composition to further elucidate the effect of microtopography on belowground CH₄ cycling.

2 Materials and Methods

2.1 Site Description

Sallie's Fen (43°12.5'N, 71°3.5'W) is located in Barrington, New Hampshire, USA approximately 20 km from the University of New Hampshire. It is a mineral-poor fen, receiving water from rainfall, run-off, and an ephemeral stream that runs along its northern edge. The growing season extends from late April to October, with deciduous plant senescence beginning in September. The water table at Sallie's Fen sits below the peat surface throughout the growing season, with an average seasonal depth of 10 to 25 cm from May to August (Treat et al., 2007; Noyce et al., 2014), dropping to 40 cm or more below the peat surface in dry years. Average daily growing season (May to September) temperature and precipitation from 2014 to 2020 was 21.8 ± 4.2°C and 2.9 ± 2.7 mm, respectively (National Centers for Environmental Information, 2020). While overall vegetation is dominated by moss (primarily *Sphagnum* spp.), dominant vascular vegetation includes ericaceous shrubs (e.g. *Chamaedaphne calyculata*, *Vaccinium oxycoccos*, *V. corymbosum*, and *Kalmia angustifolia*), sedges (*Carex rostrata*), deciduous shrubs (e.g., *Alnus incana* ssp. *rugosa*), herbaceous perennials (e.g., *Eurybia radula*, *Maianthemum trifolium*), and deciduous trees dominated by red maple (*Acer rubrum*).

We selected 8 sample plots adjacent to an automated chamber system (Bubier et al., 2003; Goodrich et al., 2011) for analysis of belowground CH₄ cycling. Mean summer CH₄ fluxes measured via the automated system are 335.0 ± 182.6 mg CH₄ m⁻² d⁻¹ (Goodrich, 2010). These plots consisted of 4 hummock plots and 4 lawn plots (Table 1) contained within an approximately 50 m by 25 m area. The ground surface height of the hummock plots was 10-20 cm higher than lawn plots. Hummocks and lawns were categorized primarily by water table depth and secondarily by dominant vegetation. The hummock plots had a deeper water table depth during both the porewater sampling (ANOVA, F_{1,6} = 8.2, p = 0.02) and microbial sampling (F_{1,6} = 7.5, p = 0.03) campaigns described below. Vegetation cover was determined as percent cover using a 1 m² quadrat that encompassed the sampling locations for coring and porewater collection described below. While hummocks and lawns did not differ significantly in the cover of sedges (F_{1,6} = 1.26, p = 0.3) nor the total cover of shrubs and trees (F_{1,6} = 0.46, p = 0.5), the most prevalent vascular plants in hummocks were ericaceous shrubs and red maple, while in lawns the dominant vascular plants included *C. rostrata* but not deciduous trees.

2.2 Incubations

In July 2018, one peat core from a hummock and a lawn plot were extracted to a depth of 70 cm using a 10 cm diameter PVC pipe. Prior to extracting cores, dissolved oxygen was measured at 10, 20, 30, 40, and 60 cm with a Hanna Instruments portable dissolved oxygen meter (HI9142). The water table level was > 10 cm below the peat surface in the hummock selected for coring, so there is no dissolved oxygen measurement for this depth. Each core was segmented into depth intervals of 10-20 cm, 30-40 cm, and 60-70 cm and sub-sampled in triplicate for both oxic and anoxic incubations. Peat coring for incubation experiments was limited to one core per microform type to reduce further disturbance to the area containing the active automated chamber system at Sallie's Fen. As such, comparisons of potential CH₄ production and oxidation and dissolved oxygen measurements are discussed as differences between the two cores/plots, not between microforms across the study site.

Peat samples were refrigerated overnight and incubation experiments began within 24 hours of field sampling. Incubations were conducted following the methodology in Perryman et al. (2020). Briefly, for oxic incubations approximately 35 g of peat was sealed into a 236 ml mason jar outfitted with a silicon septa and sealant. Jars were flushed with 0.5% CH₄ in air to give all oxic incubations a starting headspace concentration of 5000 ppm CH₄ while maintaining an oxic headspace. For anoxic incubations, approximately 15 g of peat was sealed into 200 ml glass serum vials topped with a silicon septa and crimp top. Serum vials were flushed with ultra-pure N₂ for 5 minutes to generate an anoxic headspace. All incubations were conducted at 21.5 ± 1.0 °C in dark incubators. Ten ml of headspace gas was sampled from the oxic incubation using a polypropylene syringe equipped with a three-way stopcock and replaced with 10 ml of ambient air to maintain constant pressure. Samples were taken at 2, 4, 6, 8, 24, and 48 hours after the start of the incubation period. Sample collection from the anoxic incubations began after 8 hours to allow for the accumulation of detectable CH₄ in the incubation headspace. Ten ml of headspace gas was sampled from the anoxic incubations at 8, 24, 48, 72, 96, and 120 hours after the start of the incubation period and was replaced with 10 ml of N₂ to maintain constant pressure.

Headspace gas samples were analyzed on a Shimadzu GC- 14A gas chromatograph equipped with a flame ionization detector (GC-FID). The GC-FID was operated with detector and injector temperatures of 130 °C, 50 °C column temperature, and an ultra high purity nitrogen carrier gas flow rate of 30 mL min⁻¹ through a 2-m 1/8 inch o.d. stainless steel packed column (HayeSepQ 100/120). The GC-FID was calibrated using standards of 2.51 ppm CH₄ (for the first 48 hours of anoxic incubations) and 1000 ppm CH₄ (Scott Specialty Gases, Plumsteadville, Pennsylvania; for all oxic incubations and samples from 72-120 hours of anoxic incubations). The 2.51 ppm standard was a breathing air cylinder calibrated against standards from NOAA's Earth System Research Laboratory's Global Monitoring Division's Carbon Cycle Greenhouse Gases Group.

Methane consumption was calculated as the linear decrease in CH₄ concentration over the incubation period. We restricted our calculations to the linear decrease to reflect substrate saturated conditions in which CH₄ is non-limiting to measure maximum CH₄ uptake under the incubation conditions (Sundh et al., 1995; Whalen et al., 1992). Similarly, CH₄ production was calculated using the linear increase in CH₄ concentration over the incubation period. Potential CH₄ oxidation and production rates were normalized to the dry weight of the corresponding peat sample, and converted from ppm CH₄ h⁻¹ to μmol CH₄ g_{dw}⁻¹ d⁻¹ for data analysis using:

$$\mu\text{mol CH}_4 \text{ g}_{\text{dw}}^{-1} \text{ d}^{-1} = \Delta * P * R^{-1} * T^{-1} * V * \text{g}_{\text{dw}}^{-1} * 24 \text{ h d}^{-1} \quad (\text{Eq. 1})$$

where Δ is the change in CH₄ concentration (in ppm) per hour, P is pressure in atm, R is the ideal gas constant (in L atm mol⁻¹ K⁻¹), T is the incubation temperature in K, V is the headspace volume of the incubation jar in L, and g_{dw} is the dry weight of peat.

2.3 Porewater Sampling and Analysis

Porewater samples were collected at 10, 30, and 60 cm below peat surface using a 3 mm inner diameter stainless steel sipper. Porewater samples were collected at all 8 plots on 3 sampling dates in July and August 2020. Due to variations in the water table and the presence of sapric peat at depth that prevented porewater extraction using a sipper, all 3 depths were not always retrieved from all 8 plots. Porewater samples were analyzed for pH and redox potential (Eh) on the day of sampling. Porewater collected for analysis of CH₄ concentration and CH₄ isotopes were refrigerated overnight and analyzed the following day.

Eh and pH were measured at all 3 porewater sampling depths. Redox potential was measured with an OMEGA ORP-5041 oxidation-reduction potential (ORP) electrode. The ORP electrode was calibrated using a 220 mV standard solution. Redox potential measurements were corrected for pH by standardizing to a pH of 7 by subtracting 58 mV for every pH unit below 7 (Wetzel, 2001). pH was measured using an Oakton pHTester® 50 calibrated with a 3-point calibration using standard solutions for pH 4, 7, and 10 provided by the manufacturer. Both the Eh and pH electrodes were calibrated prior to each sample collection.

For each sample, two 30 ml aliquots of porewater were equilibrated with 30 ml of ambient air in a 60-ml syringe by shaking each syringe for 2 minutes (McAuliffe, 1971). The resulting equilibrated gas was analyzed for CH₄ concentration using GC-FID as described above, as well as for isotopic analysis. The $\delta^{13}\text{C-CH}_4$ and $\delta\text{D-CH}_3\text{D}$ values of porewater CH₄ were measured using an Aerodyne dual Tunable Infrared Laser Direct Absorption Spectroscopy (TILDAS) analyzer at UNH. These instruments use high resolution infrared spectrometry to quantify trace gases such as CH₄, CO, N₂O, CO₂, NO, NO₂, and other species (McManus et al., 2011; 2015). The analyzer utilized here is configured with two 8 micron quantum cascade lasers (QCLs, Alpes Lasers) and a 200m multipass absorption cell to simultaneously monitor ¹²CH₄, ¹³CH₄, and CH₃D. The instrument precision was 0.1‰ and 3‰ for $\delta^{13}\text{C-CH}_4$ and $\delta\text{D-CH}_3\text{D}$, respectively, at the target methane mixing ratio (8 ppm). The TILDAS was regularly calibrated with three standard tanks with known isotopic mixing ratios for both ¹³CH₄/¹²CH₄ and CH₄/CH₃D. The isotopic composition of the standards tanks was determined using an Aerodyne calibration system. The spectroscopic isotope ratios of 4 Isometric (now Airgas) methane isotope standards were measured at diluted concentrations ranging from <1 to 12 ppm. A Keeling plot analysis was used to determine the relationship between the spectroscopic and standard isotope ratios of the Isometric standards. The linear relationship was then applied to the corresponding measured spectroscopic isotopic ratios of the UNH calibration tanks.

The TILDAS was configured with an automated sampling system designed to measure both high concentration samples as well as samples with CH₄ concentrations close to ambient levels. Samples can be introduced via manual injections or from attached flasks. As such, small (5 ml or less) injections of equilibrated porewater samples are diluted to the target methane mixing ratio with ultra zero air within the instrument via the sampling system program. Samples of porewater equilibrated gas were measured twice on the TILDAS and the average of the measurements was used in statistical analysis and data visualization. Some porewater samples with low CH₄ concentration (< 0.01 mM CH₄) required larger volumes of sample than was

available to reach the target mixing ratio for isotopic analysis. These datapoints were removed prior to statistical analysis.

2.4 Microbial Sampling and Analysis

In August 2014, a 70 cm deep peat core from each of the 8 sample plots was collected using a 10-cm PVC corer. The 10–20 cm, 30–40 cm, and 60–70 cm depth increments from each core were kept on ice in the field, stored frozen and shipped on dry ice to the US Forest Service Northern Research Station in Houghton, Michigan where they were stored at -20°C until further processing. DNA extraction, purification, and sequencing were performed as described in Wang et al. (2019). Briefly, 10 cm³ of peat from each sample was subsampled into a 50 ml falcon tube with twenty 3.2 mm chrome-steel beads and pulverized for 2 minutes in a modified mini-beadbeater-96. Total DNA was extracted from 0.5 g of the pulverized peat using the MoBio (now QIAGEN) Laboratories PowerSoil® DNA Isolation Kit followed by the MoBio PowerClean® kit. Extraction and purification followed the manufacturer's protocol with an additional heating step (65 °C for 30 min) during DNA extraction after bead beating. PCR library preparation and sequencing followed standard Joint Genome Institute protocols for Illumina MiSeq community amplicon sequencing (iTag; e.g., Tremblay et al. 2015; <https://jgi.doe.gov/user-programs/pmo-overview/protocols-sample-preparation-information/>), which were slightly modified from Caporaso et al. (2012). The 16S V4 region of bacteria and archaea was amplified using the primers 515F and 806R (Caporaso et al. 2012) in 25ul reactions (12ul PCR grade H2O, 10ul of 5 PRIME HotMasterMix, 1.0 ul BSA, 0.5 ul of each 10uM [] primer, and 1 ul template DNA) using the following thermocycler parameters: initial denaturation at 94 °C for 3 min, followed by 30 cycles of 94 °C for 45s, 50 °C for 60s, and 72 °C for 90s, and finally 72 °C for 10 min then holding at 4 °C. PCR reactions were performed in triplicate and pooled prior to amplicon clean-up and sequencing. PCR amplicons for each sample were sequenced using the Illumina MiSeq platform by the US Department of Energy's Joint Genome Institute (JGI). One sample from a hummock at 30–40 cm depth failed to sequence and is excluded from the analyses presented in this study. The raw sequence data have been submitted to the National Center for Biotechnology Information (NCBI) Sequence Read Archive under accession number PRJNA764764.

Sequence processing and analysis were performed using QIIME 1 1.9.1 (Caporaso et al., 2010) and QIIME 2 2019.4 (Bolyen et al. 2019). Forward and reverse reads of the interleaved raw sequence data were extracted using the `extract_reads_from_interleaved_file.py` command from QIIME1. Sequences were trimmed to remove primers and truncated at the length where the median Phred score (quality score) fell below 30 (255 bp for forward read; 200 bp for reverse read) using DADA2 (Callahan et al. 2016). The resulting merged sequences had a 164 bp overlap. Merged sequences were quality filtered and assembled into error-corrected amplicon sequence variants (ASVs) using DADA2 (via `q2-dada2`). Samples were rarefied to the maximum depth possible to retain all samples (59,181 sequences per sample), maintaining 78.65% of the ASVs. Taxonomy was assigned to ASVs using the `q2-feature-classifier` `classify-sklearn` naïve Bayes taxonomy classifier (Bokulich et al. 2018; Pedregosa et al., 2011) against the Silva v.132 99% OTUs reference sequences (Quast et al., 2013). Sequences classified as “mitochondria”, “chloroplast,” and/or those not assigned at the phylum level were removed from the dataset.

2.5 Statistical Analyses:

Further sequence processing, statistical analysis, and data visualization were performed in R v4.0.3. The level of significance for all analyses was 0.05. Data and analyses were visualized using ggplot2 (Wickham, 2016). Sequence read counts were transformed into relative abundances using the `make_relative` command from the `funrar` package (Grenié et al., 2017). ASVs were screened for known methanotrophic and methanogenic lineages to generate a curated matrix for nonmetric multidimensional scaling (NMDS) and comparison of methanotroph and methanogen total relative abundance between microforms and depth. Methanotrophs were identified based on classification into one of the following groups known to be predominantly methanotrophic: order Methyloacidiphilales, families *Methylococcaceae*, *Methylocystaceae*, and *Methylomonaceae*, and methanotrophic genera within the *Beijerinckiaceae* family (Knief, 2015; Smith & Wrighton, 2019). Methanogens were identified based on classification into one of the following orders known to be dominated by methanogens: Methanobacteriales, Methanocellales, Methanomicrobiales, Methanosarcinales, Methanomethyliales, and Methanomassiliicoccales (Evans et al., 2019; Vanwonterghem et al., 2016).

Differences in porewater pH, Eh, dissolved CH₄ concentration, $\delta^{13}\text{C-CH}_4$, and $\delta\text{D-CH}_3\text{D}$, as well as total methanotroph relative abundance, total methanogen relative abundance, and the ratio of methanotrophs to methanogens across depth and microforms were examined by mixed effects models using the `lmerTest` package (Kuznetsova et al., 2017). The mixed effects models included depth, microform (hummock vs. lawn), and their interaction as fixed effects and the plot ID as a random effect. Fixed effects were tested with the Satterthwaite approximation. Pairwise comparisons were conducted using the `emmeans` package (Lenth, 2018).

NMDS was performed on the curated matrix of methanotrophic and methanogenic lineages using Bray-Curtis distance using the `vegan` package (Oksanen et al., 2019). Biplot vectors of environmental conditions (distance to water table, percent cover of *C. rostrata*, percent cover of shrubs and trees, and porewater Eh and pH) were fit to the NMDS of methanogenic and methanotrophic lineages using the `envfit` function from the `vegan` package. Permutational multivariate analysis of variance (PERMANOVA) was performed using Bray-Curtis distance to compare dissimilarities of microbial communities within and between depths and microforms, also using the `vegan` package.

We used linear mixed effects models (LME) to assess the impact of microbial community composition, vascular vegetation, and porewater chemistry on porewater $\delta^{13}\text{C-CH}_4$, $\delta\text{D-CH}_3\text{D}$, and dissolved CH₄ concentration. The LME were performed using the mean CH₄ isotope values and concentrations from each depth at the 8 sample plots. LME were constructed using the `lmerTest` package. The LME tested the individual fixed effects of microbial (relative abundance of methanotrophs, relative abundance of methanogens, ratio of the relative abundance of methanotrophs to methanogens, and ratio of the relative abundance of acetoclastic methanogens to hydrogenotrophic methanogens), vegetation (percent cover of *C. rostrata* and percent cover of shrubs and trees), and abiotic (porewater Eh and pH) factors. For the LME models testing the fixed effect of the ratio of the relative abundance of acetoclastic methanogens to hydrogenotrophic methanogens, we consider both obligate and facultative acetoclastic methanogens (families *Methanosaetaceae* and *Methanosarcinaceae*, respectively) as acetoclastic. Plot ID was included as a random effect in all LME. We determined the amount of variance explained by just the fixed effect (marginal, R^2_m) and together with the random effect

(conditional, R^2_c) using the MuMIn package (Barton, 2019). In the main manuscript text and figures we report R^2_m .

The temporal mismatch between the microbial sampling and the porewater sampling may inherently weaken some of the observed relationships between porewater chemistry and microbial community composition. To lessen further discrepancy, we ensured that during both sampling intervals the water table was lower in hummocks than in lawns (Table 1). We recognize there is some variation in the absolute position of the water table between the two sampling intervals; as such we focus our interpretation on the impact of the relative position of the water table (hummocks lower than lawns) rather than the absolute position. Both the microbial sampling and the porewater sampling were conducted at the peak of the growing season (mid-July to mid-August) limiting the differences between the two sampling campaigns due to seasonally variable factors like primary productivity and root exudation that impact CH_4 cycling by mediating the availability of substrates for CH_4 production and oxidation (Chanton et al., 2008). We opted to use the average values from the three porewater collections (i.e. three dates between July – August for each) when analyzing these data alongside microbial data to limit the influence of possible intra-seasonal variability in porewater chemistry on the interpretation of our results.

3 Results

3.1 Potential CH_4 Production and Oxidation Rates:

The lawn and hummock cores displayed differing depth profiles of potential CH_4 production and oxidation rates. Production potential increased from $0.036 \pm 0.11 \mu\text{mol CH}_4 \text{ g}_{\text{dw}}^{-1} \text{ d}^{-1}$ at 60 cm to $3.08 \pm 0.8 \mu\text{mol CH}_4 \text{ g}_{\text{dw}}^{-1} \text{ d}^{-1}$ at 10 cm in the lawn core, while in the hummock core potential CH_4 production rates decreased from $0.56 \pm 0.21 \mu\text{mol CH}_4 \text{ g}_{\text{dw}}^{-1} \text{ d}^{-1}$ at 60 cm to $0.03 \pm 0.02 \mu\text{mol CH}_4 \text{ g}_{\text{dw}}^{-1} \text{ d}^{-1}$ at 10 cm (Figure 1a, Table S1). The difference in potential CH_4 production rates between the lawn and hummock cores was greatest at 10 cm where the highest rates of CH_4 production were observed in the lawn core and the lowest rates CH_4 production were observed in the hummock core. Mean potential CH_4 oxidation rates were more consistent across depth in the hummock core ($32.13 \pm 5.67 \mu\text{mol CH}_4 \text{ g}_{\text{dw}}^{-1} \text{ d}^{-1}$ across all depths), while in the lawn core mean rates of CH_4 oxidation decreased with depth from $29.11 \pm 6.73 \mu\text{mol CH}_4 \text{ g}_{\text{dw}}^{-1} \text{ d}^{-1}$ at 10 cm to $10.82 \pm 1.92 \mu\text{mol CH}_4 \text{ g}_{\text{dw}}^{-1} \text{ d}^{-1}$ at 60 cm (Figure 1b, Table S1). During core collection, porewater dissolved oxygen concentrations in the hummock were larger than in the lawn in the upper 30 cm (Figure 1c). Maximum dissolved oxygen concentration in the hummock was 2.7 mg L^{-1} at 20 cm, with a minimum of 0.6 mg L^{-1} at 40 cm. In the lawn maximum dissolved oxygen was 1.3 mg L^{-1} at 10 cm, and dissolved oxygen was less than 1.0 mg L^{-1} starting at 20 cm, with a minimum of 0.3 mg L^{-1} at 60 cm.

3.2 Porewater Chemistry: pH, Eh, Dissolved CH_4 , and Porewater $\delta^{13}\text{C-CH}_4$ and $\delta\text{D-CH}_3\text{D}$

Porewater pH ranged from 3.97 to 5.23 and was not significantly different between microforms but was significantly different between sampling depths. Across both hummocks and lawns pH increased with depth ($F_{2,48} = 72.3$, $p < 0.001$; Table S2). Porewater Eh ranged from 59.87 to 156.44 mV and was significantly different between both depths and microforms. Eh

decreased with depth ($F_{2,54} = 5.98$, $p = 0.005$; Table S2) and was generally higher in hummock profiles than lawn profiles ($F_{1,54} = 5.84$, $p = 0.019$; Table S2).

Dissolved CH_4 concentrations ranged from 1.5×10^{-3} to 0.59 mM and differed between sample depths ($F_{2,48} = 18.3$, $p < 0.001$, Table S2). Dissolved CH_4 concentration was highest at 30 cm in both the hummock and lawn plots (Figure 2a). The $\delta^{13}\text{C}-\text{CH}_4$ value of dissolved CH_4 ranged from -75.21‰ to -37.46‰ and differed between hummocks and lawns and by sampling depths. In both hummock and lawn plots, porewater $\delta^{13}\text{C}-\text{CH}_4$ values were highest at 10 cm ($F_{2,44} = 26.1$, $p < 0.001$; Figure 2b, Table S2). Porewater $\delta^{13}\text{C}-\text{CH}_4$ values were higher across depths in the hummock plots than the lawn plots ($F_{2,7} = 8.9$, $p = 0.02$; Figure 2b, Table S2). The hummock and lawn plots also exhibited different patterns in $\delta^{13}\text{C}-\text{CH}_4$ through the depth profile ($F_{2,44} = 3.7$, $p = 0.03$). In the hummock plots, porewater $\delta^{13}\text{C}-\text{CH}_4$ increased significantly between 60 cm and 30 cm as well as between 30 cm and 10 cm. In the lawn plots, porewater $\delta^{13}\text{C}-\text{CH}_4$ only increased significantly between 30 cm and 10 cm. Porewater $\delta\text{D}-\text{CH}_3\text{D}$ ranged from -365.6 to -115.5‰ . Porewater $\delta\text{D}-\text{CH}_3\text{D}$ values did not vary between microforms, depth, nor the interaction of these factors (Fig. 2c, Table S2)

Overall, porewater $\delta^{13}\text{C}-\text{CH}_4$ and $\delta\text{D}-\text{CH}_3\text{D}$ show a weak positive relationship ($R^2_m = 0.11$, $F_{1,51} = 6.55$, $p = 0.013$). Average $\delta^{13}\text{C}-\text{CH}_4$ and $\delta\text{D}-\text{CH}_3\text{D}$ of porewater from 10 cm in hummocks was higher than the rest of the sample depths in both hummocks and lawns (Figure 3a). Porewater $\delta^{13}\text{C}-\text{CH}_4$ values increased as dissolved CH_4 concentration decreased towards the peat surface ($R^2_m = 0.30$, $F_{1,49} = 26.2$, $p < 0.001$; Fig. 3b). Porewater $\delta\text{D}-\text{CH}_3\text{D}$ and dissolved CH_4 concentration also had a negative relationship (Figure S1, $R^2_m = 0.07$, $F_{1,46} = 5.9$, $p = 0.02$), but the relationship was much weaker than that between porewater $\delta^{13}\text{C}-\text{CH}_4$ and dissolved CH_4 concentration.

3.3 Community composition of methanogens and methanotrophs

The dominant methanotrophic genus across all samples was *Methylocystis* ($2.3 \pm 2.2\%$), which are members of the Methylocystaceae family (Figure S2). The dominant methanogens across all samples were the hydrogenotrophic genera *Methanobacterium* ($0.34 \pm 0.4\%$) and *Methanoregula* ($0.31 \pm 0.3\%$) (Figure S3). The total relative abundance of methanotrophs and methanogens varied between sampling depths but not between microforms (Table S2). The relative abundance of methanotrophs was highest at 30 cm ($F_{2,17} = 4.5$, $p = 0.027$, Table S2, Figure S2). The relative abundance of methanogens was significantly lower at 10 cm than at 30 and 60 cm ($F_{2,17} = 11.5$, $p < 0.001$, Table S2, Figure S3). The ratio of the relative abundance of methanotrophs to methanogens varied strongly by depth and was highest at 10 cm ($F_{2,16} = 10.3$, $p = 0.001$, Figure 4a, Table S2), but this depth effect depended upon microform (Microtopography \times Depth, $F_{2,16} = 3.9$, $p = 0.04$, Table S2). In lawn plots, the ratio of the relative abundance of methanotrophs to methanogens was not significantly different between depths; however, in the hummocks the ratio of the relative abundance of methanotrophs to methanogens was significantly higher at 10 cm than 30 cm and 60 cm. Overall, the highest ratio of the relative abundance of methanotrophs to methanogens was at 10 cm in the hummocks.

The community composition of methanogens and methanotrophs varied significantly between sampling depths (PERMANOVA, $F = 8.33$, $R^2 = 0.44$, $p = 0.002$), but not between hummocks and lawns ($F = 1.59$, $R^2 = 0.04$, $p = 0.17$, Figure 4b). There was not a significant effect of the interaction of microform and depth on the community composition of methanogens and methanotrophs ($F = 1.29$, $R^2 = 0.07$, $p = 0.23$). Environmental vectors were fit to the NMDS ordination, and the significance of their fit was tested using permutations of the environmental data. Neither the cover of sedges nor woody vegetation were strong correlates of the NMDS

ordination of methanotrophic and methanogenic lineages. The distance between the sample depth and the water table was the strongest environmental correlate of the NMDS ordination ($p = 0.001$), followed by pH ($p = 0.001$) and Eh ($p = 0.014$) which both vary with depth (Table 1). The strong fit between distance to the water table and the NMDS ordination reflects overall trends in the relative abundance of methanogens and methanotrophs. The relative abundance of methanogens increased with depth below the water table ($R^2_m = 0.41$, $F_{1,21} = 15.7$, $p < 0.001$, Figure S4), and the ratio of the relative abundance of methanotrophs to methanogens increased with proximity to the water table ($R^2_m = 0.32$, $F_{1,20} = 9.65$, $p = 0.0055$, Figure S4). There was no significant linear relationship between the depth below the water table and the relative abundance of methanotrophs ($R^2_m = 0.1$, $F_{1,21} = 0.3$, $p = 0.64$, Figure S4).

3.4 Controls of Porewater CH₄ Concentration and Isotopes

We used linear mixed effects models (LME) to identify potential controls of porewater $\delta^{13}\text{C-CH}_4$, $\delta\text{D-CH}_3\text{D}$, and dissolved CH₄ concentration. We grouped potential controls into three categories: microbial (relative abundance of methanotrophs, relative abundance of methanogens, ratio of the relative abundance of methanotrophs to methanogens, and ratio of the relative abundance of acetoclastic methanogens to hydrogenotrophic methanogens), vegetation (proportion of sedge and woody vegetation cover), and abiotic (Eh and pH). A full summary of the results for all LME can be found in Table S3.

Microbial controls had the strongest relationships with porewater $\delta^{13}\text{C-CH}_4$. Mean porewater $\delta^{13}\text{C-CH}_4$ increased as the ratio of the relative abundance of methanotrophs to methanogens increased ($R^2_m = 0.44$, $p = 0.0017$; Figure 5a.). Conversely, we found a negative relationship between porewater $\delta^{13}\text{C-CH}_4$ and the ratio of the relative abundance of acetoclastic methanogens to hydrogenotrophic methanogens ($R^2_m = 0.34$, $p = 0.005$; Figure 5b). Abiotic factors also had significant relationships with porewater $\delta^{13}\text{C-CH}_4$ (Figure S5, Table S3), with porewater $\delta^{13}\text{C-CH}_4$ increasing as Eh increased ($R^2_m = 0.27$, $p = 0.016$) and pH decreased ($R^2_m = 0.25$, $p = 0.012$). There was not a significant relationship between porewater $\delta^{13}\text{C-CH}_4$ and the proportion of sedge nor woody vegetation cover (Figure 5c-d). We also did not observe significant relationships between porewater $\delta\text{D-CH}_3\text{D}$ and any of the potential microbial, vegetation, or abiotic controls.

Microbial controls also had the strongest relationships with dissolved CH₄ concentration. Dissolved CH₄ concentration had a positive relationship with the relative abundance of both methanotrophs ($R^2_m = 0.24$, $p = 0.009$) and methanogens ($R^2_m = 0.16$, $p = 0.015$) and a negative relationship with the ratio of the relative abundance of methanotrophs to methanogens ($R^2_m = 0.17$, $p = 0.03$). There were no significant relationships between dissolved CH₄ concentration and any of the potential vegetation or abiotic controls.

4 Discussion

4.1 Contrasting Dominant CH₄ Cycling Processes in Hummocks and Lawns

Using profiles of potential CH₄ production and oxidation from incubations, dissolved CH₄ concentration, and porewater $\delta^{13}\text{C-CH}_4$ and $\delta\text{D-CH}_3\text{D}$ as a proxy for methanogenic and methanotrophic activity, we observed diverging CH₄ cycling processes in the hummock and lawn plots. The hummock core had high CH₄ oxidation potential across depth (Figure 1b), while in the lawn core potential CH₄ oxidation nearly doubled from 30 cm to 10 cm (Table S1). These results are consistent with previous work that observed higher rates of potential CH₄ production

in the surface peat of saturated microforms and higher rates of potential CH₄ oxidation at depth in more aerated hummocks (Juottonen et al., 2015). Taken together, our incubation results show that methanotrophs readily oxidized CH₄ across depth in the hummock core, while in the lawn core methanotrophs responded to substrate availability (e.g., high rates of CH₄ production), closer to the peat surface. While our inferences about CH₄ production and oxidation potential from incubations are limited due to our sample size, we were able to make inferences about processes based on these incubations. Furthermore, incubations indicate potential, not realized, rates of CH₄ production and oxidation. As such, additional measurements were needed to solidify our inferences about *in situ* processes across microforms. We more deeply explored patterns of methanogenic and methanotrophic activity using porewater geochemical proxies, which were more highly replicated across the site and more reflective of *in situ* activity.

While the hummocks and lawns had similar profiles of dissolved CH₄ concentration (Figure 2a), porewater $\delta^{13}\text{C}\text{-CH}_4$ values from the hummocks and lawns indicate differing dominant microbial CH₄ cycling processes occurring *in situ* across depth between these microforms. Porewater $\delta^{13}\text{C}\text{-CH}_4$ did not differ between hummocks and lawns at 60 cm, as previously observed in a Finnish boreal peatland where porewater $\delta^{13}\text{C}\text{-CH}_4$ did not vary between hummocks, lawns, and hollows below 50 cm (Dorodnikov et al., 2013). However, above 60 cm porewater $\delta^{13}\text{C}\text{-CH}_4$ was significantly higher in hummocks than lawns (Figure 2b), which may be due to increased methanotrophy in the hummocks as oxidation causes residual CH₄ to become enriched in ¹³C (Coleman et al., 1981). Porewater $\delta^{13}\text{C}\text{-CH}_4$ in the lawn plots was ~10‰ lower than in hummocks at both 10 cm ($-59.29 \pm 6.23\text{‰}$ and $-49.56 \pm 8.42\text{‰}$, respectively) and 30 cm ($-67.58 \pm 4.16\text{‰}$ and $-58.89 \pm 3.24\text{‰}$, respectively) and more reflective of methanogenesis than methanotrophy (Chanton et al., 2005; Whiticar, 1999).

While porewater $\delta\text{D}\text{-CH}_3\text{D}$ values lacked clear trends with respect to microtopography and depth (Figure 2c), they were informative for further differentiating dominant CH₄-cycling processes when interpreted alongside porewater $\delta^{13}\text{C}\text{-CH}_4$. In hummocks, mean porewater $\delta\text{D}\text{-CH}_3\text{D}$ increases ~60‰ from 30 cm to 10 cm. This increase in porewater $\delta\text{D}\text{-CH}_3\text{D}$ coincides with a ~10‰ increase in porewater $\delta^{13}\text{C}\text{-CH}_4$ (Figure 3a, Table S1). Dual isotopic enrichment of ¹³C and D in dissolved CH₄ in the surface of the hummocks further supports that CH₄ is oxidized *in situ* in the aerated upper portion of the peat profile in hummocks (Coleman et al., 1981; Whiticar, 1999). This dual isotopic enrichment is not observed in the lawns where the patterns of porewater $\delta^{13}\text{C}\text{-CH}_4$ and $\delta\text{D}\text{-CH}_3\text{D}$ observed across depth indicate that methanogenesis dominates the isotopic signal (Figure 3a, Chanton et al., 2005).

Our geochemical observations indicate that differences in water table position across hummocks and lawns strongly influence belowground CH₄ cycling by mediating belowground redox conditions. Redox potential was higher throughout the profile in hummocks than in lawns (Table 1, Table S2), and Eh also had a significant positive relationship with porewater $\delta^{13}\text{C}\text{-CH}_4$ (Table S3, Figure S5). Prior research on controls of CH₄ cycling in northern peatlands indicates that Eh is a strong control of methanotrophy (Perryman et al., 2020; Rupp et al., 2019); therefore, the more oxidizing conditions in hummocks may be promoting greater methanotrophic activity than in lawns. While the porewater sampling for this study targeted the peak of the growing season at Sallie's Fen, Kato et al. (2013) measured porewater $\delta^{13}\text{C}\text{-CH}_4$ across hummocks and more saturated hollows in an alpine wetland in both summer and fall and similarly observed that surface porewater $\delta^{13}\text{C}\text{-CH}_4$ was larger in the hummocks (~ -50 to -55‰) than the hollows (~ -60 to -65‰). Consistent with our study, the difference in porewater CH₄ isotope composition between microforms observed by Kato et al. (2013) was largely driven by the position of the

water table. Shoemaker et al. (2012) observed that porewater $\delta^{13}\text{C}\text{-CH}_4$ ranged from approximately -54 to -63‰ in samples collected from Sallie's Fen in July through December. While this range is in good agreement with the average porewater $\delta^{13}\text{C}\text{-CH}_4$ values we observed at the peak of the growing season (Table S2), Shoemaker et al. (2012) reported too few fall ($n = 3$) and winter ($n = 2$) measurements to make further comparisons to our observations.

The influence of vegetation on belowground CH_4 cycling is less clear in our dataset. The $\delta^{13}\text{C}\text{-CH}_4$ measurements did not indicate that the increased dominance of sedges in the lawn plots enhanced rhizospheric CH_4 oxidation (Figure 4c) as suggested by prior work in northern peatlands (Popp et al., 2000; Rupp et al., 2019; Strom et al., 2005), possibly because of the low (< 30%) density of sedges in the lawn plots. As sedges are codominant with other vegetation in the lawn plots used in this study (Table 1), the potential oxidizing effect of sedges may be outweighed by the higher water table position that is promoting methanogenesis at the peat surface in the lawn plots (Figure 1-3). While the difference in sedge abundance between the hummocks and lawns at Sallie's Fen may be too limited to affect rates of rhizospheric CH_4 oxidation, Hines et al. (2008) observed that even slight changes to the abundances of sedges over small spatial scales (~2 m) can significantly impact rates of acetate and CH_4 production. Our observation of high rates of CH_4 production (Figure 1a) and porewater $\delta^{13}\text{C}\text{-CH}_4$ and $\delta\text{D}\text{-CH}_3\text{D}$ values more indicative of acetoclastic methanogenesis (Figure 3a) near the peat surface in the lawns may reflect some difference in the quantity and quality of methanogenic substrates between the hummocks and lawns due to variation in sedge abundance.

In summary, our geochemical observations suggest that belowground CH_4 cycling in hummocks is more strongly regulated by methanotrophy, while in lawns methanogenesis is more dominant. While we did not directly measure the response of belowground CH_4 cycling in hummocks and lawns to warming, our results could inform inferences on how peatland CH_4 cycling may respond to rising temperatures. Previous evidence from both laboratory (Dunfield et al., 1993) and field (Pedersen et al., 2018) experiments indicates that CH_4 production is more temperature sensitive than CH_4 oxidation. As such, our findings suggest that net CH_4 emissions may respond to warming differently across microforms based on variation in the microbial processes regulating belowground CH_4 cycling.

4.2 Depth Stratification of Microbial Community Composition Across Microforms

Our analysis of 16S rRNA amplicon sequences indicates that the total relative abundances (Figure S2-S3, Table S2) and community composition (Figure 4b) of known methanogenic and methanotrophic lineages do not vary between hummocks and lawns at Sallie's Fen. This result is consistent with previous work showing that microtopography has limited influence on methanogenic and methanotrophic abundance and diversity in Scandinavian (Martí et al., 2015) and Patagonian peatlands (Kip et al., 2012). In studies comparing CH_4 cycling across multiple sites, inter-site variation in methanogen and methanotroph community composition is often larger than variation between microforms within the same field site, possibly due to site-specific geoclimatological conditions (Martí et al., 2015) or substrate availability unrelated to microform-specific vegetation inputs (Juottonen et al., 2015). Differences in microbial community composition across microforms may also be more pronounced when microforms have more distinct vegetation communities. For example, Chroňáková et al. (2019), found that hummocks dominated by blueberry (*V. myrtillus*), *Eriophorum* dominated lawns, and *Sphagnum*-dominated hollows found in spruce swamp forests in the Czech Republic harbored unique microbial communities, including methanotrophs and methanogens. Furthermore, Lamit et al. (2021)

observed that changes in CH₄-cycling microbial lineages in a vegetation removal experiment were mediated by water table depth. For example, sedge removal generally decreased methanotroph relative abundance, but removing *Ericaceae* increased methanotroph relative abundance under high water table conditions but reduced methanotroph relative abundance under low water table conditions (Lamit et al., 2021). The hummocks and lawns at Sallie's Fen have similar dominant vascular vegetation (Table 1), and so the linkage between aboveground vegetation and belowground microbial communities is less clear at our study site.

We do find that the relative abundance and community composition of methanotrophs and methanogens varies strongly between sample depths (Figure S2-S3, Figure 4b), and that this variation is related to environmental conditions like pH, Eh, and the distance from the water table (Figure 4b, Figure S4). As methanotrophs and methanogens occupy distinct redox niches (Bodelier et al., 2013; Conrad, 2007; Knief, 2015), vertical stratification of methanotrophs and methanogens is commonly observed in peatlands. For example, microbial functional groups were vertically stratified across hummocks and hollows in a poor fen in Ontario (Asemaninejad et al., 2019), where the surface (0-5 cm) of hummocks was characterized by aerobic methanotrophs while the lower depths (30-35 cm) of saturated hollows were characterized by methanogens. We observed vertical stratification in the total relative abundance of methanotrophs and methanogens across all plots, regardless of microtopography, with methanotroph relative abundance peaking near the maximum seasonal depth of the water table (approximately 30 cm), below which methanogens become significantly more abundant (Figure S3).

Notably, we did find that the surface peat of hummocks had a significantly larger ratio of the relative abundance of methanotrophs to methanogens than lawns (Figure 4a, Table S2). The difference in the ratio of the relative abundance of methanotrophs to methanogens at 10 cm between microforms is due to the lower relative abundance of methanogens at this depth in hummocks than lawns ($0.031 \pm 0.038\%$ vs $0.23 \pm 0.14\%$, respectively, Fig. S3), consistent with our observations of lower water table depth in hummocks (Table 1) and a decrease in the relative abundance of methanogens with distance above the water table (Fig. S4). As such, the lower water table position in the hummocks promotes conditions more favorable to aerobes than anaerobes at the peat surface, further skewing the microbial community towards methanotrophs.

4.3 Controls of CH₄ Cycling Across Microforms: Water Table Depth vs. Vegetation

Identifying controls on the isotopic composition of CH₄ can provide important insight into the processes regulating CH₄ cycling, as $\delta^{13}\text{C-CH}_4$ integrates a variety of fractionating biological and transport processes. Our results indicate that the ratio of the relative abundance of methanotrophs to methanogens is the strongest predictor of porewater $\delta^{13}\text{C-CH}_4$ (Figure 5a, Table S3), with porewater $\delta^{13}\text{C-CH}_4$ increasing as the ratio of methanotrophs to methanogens increased. We found a similarly strong relationship between porewater $\delta^{13}\text{C-CH}_4$ and the ratio of acetoclastic to hydrogenotrophic methanogens (Figure 5b); however, our results show porewater $\delta^{13}\text{C-CH}_4$ decreasing as the ratio of the relative abundance of acetoclastic to hydrogenotrophic methanogens increased. This result is opposite of the expected relationship, as acetoclastic methanogenesis yields higher $\delta^{13}\text{C-CH}_4$ values than hydrogenotrophic methanogenesis (Chanton et al., 2005; Whiticar, 1999), and likely reflects the larger total relative abundance of methanogens at depth (Figure S3). Microbial community composition has been similarly identified as a predictor of CH₄ cycling in other northern peatlands. In thawing permafrost peat, the relative abundance of the methanogen *Candidatus 'Methanoflorens stordalenmirensis'* was a key predictor of CH₄ isotopes (McCalley et al., 2014). In temperate bogs, both the ratio of the

relative abundance of methanogens to methanotrophs (Rey-Sanchez et al., 2019) and gene-to-transcript abundance ratios of methanogens and methanotrophs (Freitag et al., 2010) have been shown to be strong controls of CH₄ emissions. Our results further support that microbial community composition is a key regulating factor in peatland CH₄ dynamics across peatland types, climatic zones, and microtopography.

We did not observe any significant relationships between vascular vegetation composition and porewater dissolved CH₄ concentration or isotopic composition (Figure 5c-d, Table S2), consistent with our finding that vascular vegetation had no clear influence on methanogen and methanotroph community composition. Prior work at our study site similarly found little influence of vegetation composition on seasonal and interannual patterns of belowground CH₄ concentration (Shoemaker et al., 2012). We did observe strong relationships between porewater δ¹³C-CH₄ and Eh and pH (Table S3, Figure S5), consistent with the strong vertical stratification we observed in methanogen and methanotroph community composition driven by microbial redox niches. Our observations suggest that while vegetation plays a minimal role in regulating belowground CH₄ cycling across microforms at our study site, redox conditions controlled by the depth of the water table strongly influenced belowground CH₄ cycling. This conclusion holds across our geochemical and microbial observations, in which hummocks, which had a lower water table position (Table 1) and higher Eh (Table 1, Table S2) also had higher porewater δ¹³C-CH₄ values (Figure 2b) and a larger methanotroph to methanogen ratio at the peat surface than lawns (Figure 4a). Our results indicate that there can be strong differences in belowground CH₄ cycling between microforms with varying water table depth in the absence of distinct vegetation communities.

The temporal mismatch between the sampling campaigns included in this study introduces additional uncertainty to our results. While the absolute position of the water table in hummocks and lawns varied across sampling events, the water table depth during all sampling intervals was lower in hummocks than lawns (Table 1, Fig. 1c). As such, the impact of water table position on porewater CH₄ dynamics and microbial community composition was likely consistent between years. Furthermore, we conducted all sampling campaigns during the portion of the growing season (July-August) when CH₄ emissions have been observed to be at their seasonal maximum at Sallie's Fen across many studies (e.g. Carroll et al., 1997 ; Frohling & Crill, 1994 ; Goodrich et al., 2011; Treat et al., 2007), suggesting there is long-term interannual stability in the balance of CH₄ production, oxidation, and subsequent emission even if there is variation in seasonal water table levels, temperature, precipitation, etc. between years. Despite the temporal mismatch, we observed consistent patterns across our geochemical and microbial observations that informed our interpretation of controls on belowground CH₄ cycling across microforms.

Differentiating the dominant controls of belowground CH₄ cycling and CH₄ emissions is important for improving process-based wetland CH₄ models. While vegetation did not have a clear influence on belowground CH₄ cycling at our study site, vegetation likely exerts a strong control on peatland CH₄ emissions and variations in CH₄ emissions across microforms at Sallie's Fen. Previous work across northern peatlands supports the strong influence of vegetation on CH₄ emissions (e.g. Bubier et al., 1995; Frenzel & Karofeld, 2000; Moore et al., 2011), particularly of sedges with aerenchymous tissues that transport CH₄ to the atmosphere (Noyce et al., 2014; Waddington et al., 1996). Often the relationship between aboveground vegetation and CH₄ emissions is mediated by other environmental factors including water table depth (Treat et al., 2007). Our results further support that water table depth plays a key mediating role in whole-ecosystem CH₄ dynamics by changing the depth-distribution of CH₄ production and oxidation

across microforms. In peatlands where vegetation is less distinct across microforms as at Sallie's Fen (Table 1), water table depth is likely the dominant factor influencing belowground CH₄ cycling. As such, while differences in vegetation communities may be important for CH₄ emissions due to their influence on gas transport, factors that shape microbial redox niches may be more influential drivers of belowground CH₄ cycling across peatland microforms.

5 Conclusions

We observed consistent geochemical signals indicating that belowground CH₄ cycling in hummocks is more strongly regulated by methanotrophy, while in lawns methanogenesis is more dominant. While there was no significant difference in the relative abundance nor community composition of methanogens and methanotrophs between hummocks and lawns, we did observe strong vertical stratification of these microbial communities across microforms driven by the position of the water table. Notably, there was a larger ratio of the relative abundance of methanotrophs to methanogens in the surface peat of hummocks than in lawns where the water table is closer to the peat surface. The ratio of the relative abundance of methanotrophs to methanogens was a strong predictor of porewater CH₄ chemistry, suggesting that the difference in water table position across microforms influences whether CH₄ production or oxidation more strongly regulates belowground CH₄ cycling. Conversely, vegetation composition lacked a clear influence on porewater CH₄ chemistry and microbial community composition across microforms at our study site, likely due to the lack of distinct vegetation communities in hummocks and lawns.

Our results present two important considerations for understanding how peatland CH₄ cycling will respond to climate and environmental change. Firstly, the difference we observed in which microbial process regulates belowground CH₄ cycling suggests that hummocks and lawns may respond asymmetrically to warming, as previous work indicates that methanogenesis and methanotrophy have differing temperature responses. Secondly, our results suggest that, when differences between vegetation communities are relatively subtle, water table exerts a primary control of belowground CH₄ cycling across peatland microforms. The differences in regulating microbial processes across microforms and the controls of belowground CH₄ cycling are critical to consider for process-based models. Overall, our work further highlights the need to incorporate microtopography in attempts to scale up model predictions of peatland CH₄ emissions from plot to landscape level.

Acknowledgments

This work was supported by the NSF GRFP [Grant No. DGE145027], the New Hampshire Space Grant Consortium Graduate Fellowship, the USDA Forest Service Northern Research Station Climate Change Program, the NSF MacroSystems Biology Program (EF-1241937), the NASA IDS Program (NNX17AK10G), and the U.S. Department of Energy Joint Genome Institute Community Science Program [Proposal ID 1445]. The work conducted by the U.S. Department of Energy Joint Genome Institute, a DOE Office of Science User Facility, is supported by the Office of Science of the U.S. Department of Energy under Contract No. DE-AC02-05CH11231. The authors would also like to acknowledge Jack Dibb and Sallie Whitlow for allowing access to Sallie's Fen and the UNH Hamel Center for Undergraduate Research for funding field assistants Madelaine Juffras and Mike Zampini.

Open Research

The sequence data presented in this manuscript have been submitted to the National Center for Biotechnology Information (NCBI) Sequence Read Archive under accession number PRJNA764764. All other biogeochemical data presented in this manuscript are available at the Zenodo repository under “*Potential Methane Production and Oxidation Rates and Porewater Chemistry Across Peatland Hummocks and Lawns*” (<https://doi.org/10.5281/zenodo.6762592>).

References

- Asemaninejad, A., Thorn, R. G., Branfireun, B. A., & Lindo, Z. (2019). Vertical stratification of peatland microbial communities follows a gradient of functional types across hummock–hollow microtopographies. *Écoscience*, 26(3), 249–258. <https://doi.org/10.1080/11956860.2019.1595932>
- Barton, K. (2019). MuMIn: Multi-Model Inference. R package version 1.43.6. <https://CRAN.R-project.org/package=MuMIn>.
- Bodilier, P. L., Meima-Franke, M., Hordijk, C. A., Steenbergh, A. K., Hefting, M. M., Bodrossy, L., von Bergen, M., & Seifert, J. (2013). Microbial minorities modulate methane consumption through niche partitioning. *The ISME Journal*, 7(11), 2214–2228. <https://doi.org/10.1038/ismej.2013.99>
- Bokulich, N. A., Kaehler, B. D., Rideout, J. R., Dillon, M., Bolyen, E., Knight, R., ... Gregory Caporaso, J. (2018). Optimizing taxonomic classification of marker-gene amplicon sequences with QIIME 2’s q2-feature-classifier plugin. *Microbiome*, 6(1), 1–17. <https://doi.org/10.1186/s40168-018-0470-z>
- Bolyen, E., Rideout, J. R., Dillon, M. R., Bokulich, N. A., Abnet, C. C., Al-Ghalith, G. A., ... Caporaso, J. G. (2019). Reproducible, interactive, scalable and extensible microbiome data science using QIIME 2. *Nature Biotechnology*, 37(8), 852–857. <https://doi.org/10.1038/s41587-019-0209-9>
- Bubier, J., Costello, A., Moore, T.R., Roulet, N.T., & Savage, K. (1993). Microtopography and methane flux in boreal peatlands, northern Ontario, Canada. *Canadian Journal of Botany*, 71, 1056–1063.
- Bubier, J., Crill, P., Mosedale, A., Frolking, S., & Linder, E. (2003). Peatland responses to varying interannual moisture conditions as measured by automatic CO₂ chambers: Peatland responses to interannual moisture. *Global Biogeochemical Cycles*, 17(2). <https://doi.org/10.1029/2002GB001946>
- Bubier, J. L., Moore, T. R., Bellisario, L., Comer, N. T., & Crill, P. M. (1995). Ecological controls on methane emissions from a Northern Peatland Complex in the zone of discontinuous permafrost, Manitoba, Canada. *Global Biogeochemical Cycles*, 9(4), 455–470. <https://doi.org/10.1029/95GB02379>
- Callahan, B. J., Mcmurdie, P. J., Rosen, M. J., Han, A. W., Johnson, A. J. A., & Holmes, S. P. (2016). DADA2: High resolution sample inference from Illumina amplicon data. *Nature Methods*, 13(7), 581–583. <https://doi.org/10.1038/nmeth.3869>.DADA2
- Caporaso, J. G., Kuczynski, J., Stombaugh, J., Bittinger, K., Bushman, F. D., Costello, E. K., et al. (2010). QIIME allows analysis of high-throughput community sequencing data. *Nature Methods* 7, 335–336.

- Carroll, P., & Crill, P. (1997). Carbon balance of a temperate poor fen. *Global Biogeochemical Cycles*, 11(3), 349–356. <https://doi.org/10.1029/97GB01365>
- Caporaso, J. G., Lauber, C. L., Walters, W. A., Berg-Lyons, D., Lozupone, C. A., Turnbaugh, P. J., Noah Fierer, N., & Knight, R. (2011). Global patterns of 16S rRNA diversity at a depth of millions of sequences per sample. *Proc Natl Acad Sci USA*, 108, 4516–4522. <http://doi.org/10.1073/pnas.1000080107>
- Chanton, J., Chaser, L., Glasser, P., & Siegel, D. (2005). Carbon and Hydrogen Isotopic Effects in Microbial, Methane from Terrestrial Environments. In *Stable Isotopes and Biosphere Atmosphere Interactions* (pp. 85–105). Elsevier. <https://doi.org/10.1016/B978-012088447-6/50006-4>
- Chanton, J. P., Glaser, P. H., Chasar, L. S., Burdige, D. J., Hines, M. E., Siegel, D. I., Tremblay, L. B., & Cooper, W. T. (2008). Radiocarbon evidence for the importance of surface vegetation on fermentation and methanogenesis in contrasting types of boreal peatlands. *Global Biogeochemical Cycles*, 22(4). <https://doi.org/10.1029/2008GB003274>
- Chroňáková, A., Bárta, J., Kaštovská, E., Urbanová, Z., & Pícek, T. (2019). Spatial heterogeneity of belowground microbial communities linked to peatland microhabitats with different plant dominants. *FEMS Microbiology Ecology*, 95(9), fiz130. <https://doi.org/10.1093/femsec/fiz130>
- Coleman, D. D., Risatti, J. B., & Schoell, M. (1981). Fractionation of carbon and hydrogen isotopes by methane-oxidizing bacteria. *Geochimica et Cosmochimica Acta*, 45(7), 1033–1037. [https://doi.org/10.1016/0016-7037\(81\)90129-0](https://doi.org/10.1016/0016-7037(81)90129-0)
- Conrad, R. (2007). Microbial Ecology of Methanogens and Methanotrophs. In *Advances in Agronomy* (Vol. 96, pp. 1–63). Elsevier. [https://doi.org/10.1016/S0065-2113\(07\)96005-8](https://doi.org/10.1016/S0065-2113(07)96005-8)
- Crill, P. M., Bartlett, K. B., Harriss, R. C., Gorham, E., Verry, E. S., Sebacher, D. I., Madzar, L., & Sanner, W. (1988). Methane flux from Minnesota Peatlands. *Global Biogeochemical Cycles*, 2(4), 371–384. <https://doi.org/10.1029/GB002i004p00371>
- Deng, Y., Cui, X., Hernández, M., & Dumont, M. G. (2014). Microbial Diversity in Hummock and Hollow Soils of Three Wetlands on the Qinghai-Tibetan Plateau Revealed by 16S rRNA Pyrosequencing. *PLoS ONE*, 9(7), e103115. <https://doi.org/10.1371/journal.pone.0103115>
- Dorodnikov, M., Marushchak, M., Biasi, C., & Wilmking, M. (2013). Effect of microtopography on isotopic composition of methane in porewater and efflux at a boreal peatland. *Boreal Environmental Research*, 18, 269–279.
- Dunfield, P., Knowles, R., Dumont, R., & Moore, T. (1993). Methane production and consumption in temperate and subarctic peat soils: Response to temperature and pH. *Soil Biology and Biochemistry*, 25(3), 321–326. [https://doi.org/10.1016/0038-0717\(93\)90130-4](https://doi.org/10.1016/0038-0717(93)90130-4)
- Etminan, M., Myhre, G., Highwood, E. J., & Shine, K. P. (2016). Radiative forcing of carbon dioxide, methane, and nitrous oxide: A significant revision of the methane radiative forcing. *Geophysical Research Letters*, 43, 12,614–12,623. <https://doi.org/10.1002/2016GL071930>
- Evans, P.N., Boyd, J.A., Leu, A.O., Woodcroft, B.J., Parks, D.H., Hugenholtz, P., & Tyson, G.W. (2019) An evolving view of methane metabolism in the Archaea. *Nature Reviews Microbiology*, 17, 219–232. <https://doi.org/10.1038/s41579-018-0136-7>
- Freitag, T. E., Toet, S., Ineson, P., & Prosser, J. I. (2010). Links between methane flux and transcriptional activities of methanogens and methane oxidizers in a blanket peat bog: Methane flux and transcriptional activities in a peat bog. *FEMS Microbiology Ecology*, no. no. <https://doi.org/10.1111/j.1574-6941.2010.00871.x>

- Frenzel, P., & Karofeld, E. (2000). CH₄ emission from a hollow-ridge complex in a raised bog: The role of CH₄ production and oxidation. *Biogeochemistry*, *51*, 91–112.
- Frolking, S., & Crill, P. (1994). Climate controls on temporal variability of methane flux from a poor fen in southeastern New Hampshire: Measurement and modeling. *Global Biogeochemical Cycles*, *8*(4), 385–397. <https://doi.org/10.1029/94GB01839>
- Goodrich, J. P. (2010). Identifying temporal patterns and controlling factors in methane ebullition at Sallie's Fen, a temperate peatland site, using automated chambers. (Master's Thesis). Retrieved from ProQuest. (<https://www.proquest.com/docview/762169193/E9E25E1DFC184C92PQ/>). Location: University of New Hampshire.
- Goodrich, J. P., Varner, R. K., Frolking, S., Duncan, B. N., & Crill, P. M. (2011). High-frequency measurements of methane ebullition over a growing season at a temperate peatland site: Peatland CH₄ ebullition. *Geophysical Research Letters*, *38*(7), n/a-n/a. <https://doi.org/10.1029/2011GL046915>
- Granberg, G., Mikkilä, C., Sundh, I., Svensson, B. H., & Nilsson, M. (1997). Sources of spatial variation in methane emission from mires in northern Sweden: A mechanistic approach in statistical modeling. *Global Biogeochemical Cycles*, *11*(2), 135–150. <https://doi.org/10.1029/96GB03352>
- Greenup, A. L., Bradford, M. A., Mcnamara, N. P., Ineson, P., & Lee, J. A. (2000). The role of *Eriophorum vaginatum* in CH₄ flux from an ombrotrophic peatland. *Plant and Soil*, *227*(1–2), 265–272. <https://doi.org/10.1023/A:1026573727311>
- Grenié, M., Denelle, P., Tucker, C. M., Munoz, F., & Violle, C. (2017). “funrar: An R package to characterize functional rarity.” Diversity and Distributions. doi: 10.1111/ddi.12629 (URL: <https://doi.org/10.1111/ddi.12629>)
- Hines, M. E., Duddleston, K. N., Rooney-varga, J. N., Fields, D., & Chanton, J. P. (2008). Uncoupling of acetate degradation from methane formation in Alaskan wetlands: Connections to vegetation distribution. *Global Biogeochemical Cycles*, *22*, 1–12. <https://doi.org/10.1029/2006GB002903>
- Hugelius, G., Loisel, J., Chadburn, S., Jackson, R. B., Jones, M., MacDonald, G., Marushchak, M., Olefeldt, D., Packalen, M., Siewert, M. B., Treat, C., Turetsky, M., Voigt, C., & Yu, Z. (2020). Large stocks of peatland carbon and nitrogen are vulnerable to permafrost thaw. *Proceedings of the National Academy of Sciences*, *117*(34), 20438–20446. <https://doi.org/10.1073/pnas.1916387117>
- Juottonen, H., Kotiaho, M., Robinson, D., Merilä, P., Fritze, H., & Tuittila, E.-S. (2015). Microform-related community patterns of methane-cycling microbes in boreal *Sphagnum* bogs are site specific. *FEMS Microbiology Ecology*, *91*(9), fiv094. <https://doi.org/10.1093/femsec/fiv094>
- Kato, T., Yamada, K., Tang, Y., Yoshida, N., & Wada, E. (2013). Stable carbon isotopic evidence of methane consumption and production in three alpine ecosystems on the Qinghai–Tibetan Plateau. *Atmospheric Environment*, *77*, 338–347. <https://doi.org/10.1016/j.atmosenv.2013.05.010>
- Kettunen, A. (2003). Connecting methane fluxes to vegetation cover and water table fluctuations at microsite level: A modeling study. *Global Biogeochemical Cycles*, *17*(2). <https://doi.org/10.1029/2002GB001958>
- Kip, N., Fritz, C., Langelaan, E. S., Pan, Y., Bodrossy, L., Pancotto, V., Jetten, M. S. M., Smolders, A. J. P., & Op den Camp, H. J. M. (2012). Methanotrophic activity and diversity

- in different *Sphagnum magellanicum* dominated habitats in the southernmost peat bogs of Patagonia. *Biogeosciences*, 9(1), 47–55. <https://doi.org/10.5194/bg-9-47-2012>
- Knief, C. (2015). Diversity and Habitat Preferences of Cultivated and Uncultivated Aerobic Methanotrophic Bacteria Evaluated Based on *pmoA* as Molecular Marker. *Frontiers in Microbiology*, 6. <https://doi.org/10.3389/fmicb.2015.01346>
- Knorr, K.-H., & Blodau, C. (2009). Impact of experimental drought and rewetting on redox transformations and methanogenesis in mesocosms of a northern fen soil. *Soil Biology and Biochemistry*, 41(6), 1187–1198. <https://doi.org/10.1016/j.soilbio.2009.02.030>
- Krohn, J., Lozanovska, I., Kuzyakov, Y., Parvin, S., & Dorodnikov, M. (2017). CH₄ and CO₂ production below two contrasting peatland micro-relief forms: An inhibitor and $\delta^{13}\text{C}$ study. *Science of The Total Environment*, 586, 142–151. <https://doi.org/10.1016/j.scitotenv.2017.01.192>
- Lamit, L. J., Romanowicz, K. J., Potvin, L. R., Lennon, J. T., Tringe, S. G., Chimner, R. A., Kolka, R. K., Kane, E. S., & Lilleskov, E. A. (2021). Peatland microbial community responses to plant functional group and drought are depth- dependent. *Molecular Ecology*, mec.16125. <https://doi.org/10.1111/mec.16125>
- Kuznetsova, A., Brockhoff, P., & Christensen, R. (2017). lmerTest Package: Tests in Linear Mixed Effects Models. *Journal of Statistical Software*, 82(13), 1–26. <http://dx.doi.org/10.18637/jss.v082.i13>
- Lenth, R. (2018). Emmeans: estimated marginal means, aka least- squares means. R package version 1.3.0. <https://CRAN.R-project.org/package=emmeans>
- Martí, M., Juottonen, H., Robroek, B. J. M., Yrjälä, K., Danielsson, Å., Lindgren, P.-E., & Svensson, B. H. (2015). Nitrogen and methanogen community composition within and among three *Sphagnum* dominated peatlands in Scandinavia. *Soil Biology and Biochemistry*, 81, 204–211. <https://doi.org/10.1016/j.soilbio.2014.11.016>
- McAuliffe, C. (1971). Gas chromatographic determination of solutes by multiple phase equilibrium. *Chemical Technology*, 1, 46–51.
- McCalley, C. K., Woodcroft, B. J., Hodgkins, S. B., Wehr, R. A., Kim, E.-H., Mondav, R., Crill, P. M., Chanton, J. P., Rich, V. I., Tyson, G. W., & Saleska, S. R. (2014). Methane dynamics regulated by microbial community response to permafrost thaw. *Nature*, 514(7523), 478–481. <https://doi.org/10.1038/nature13798>
- McManus, J. B., Zahniser, M. S. & Nelson, D. D. (2011). Dual quantum cascade laser trace gas instrument with astigmatic Herriott cell at high pass number. *Appl. Opt.* 50, A74–85.
- McManus, J. B. et al. (2015). Recent progress in laser-based trace gas instruments: performance and noise analysis. *Applied Physics B*, 119, 203–218.
- Moore, T. R., De Young, A., Bubier, J. L., Humphreys, E. R., Lafleur, P. M., & Roulet, N. T. (2011). A Multi-Year Record of Methane Flux at the Mer Bleue Bog, Southern Canada. *Ecosystems*, 14(4), 646–657. <https://doi.org/10.1007/s10021-011-9435-9>
- National Centers for Environmental Information (2020). Climate Data Online - Daily Summaries [Data file]. Retrieved from <https://www.climate.gov/maps-data/dataset/past-weather-zip-code-data-table>
- Noyce, G. L., Varner, R. K., Bubier, J. L., & Frohling, S. (2014). Effect of *Carex rostrata* on seasonal and interannual variability in peatland methane emissions: Effect of *C. Rostrata* on CH₄ emissions. *Journal of Geophysical Research: Biogeosciences*, 119(1), 24–34. <https://doi.org/10.1002/2013JG002474>

- Oksanen, J., Blanchet, F. G., Friendly, M., Kindt, R., Legendre, P., McGlinn, D., Minchin, P.R., O'Hara, R. B., Simpson, G. L., Solymos, P., Stevens, M. H. H., Szoecs, E., & Wagner, H. (2019). *vegan: Community Ecology Package*. R package version 2.5-6. <https://CRAN.R-project.org/package=vegan>
- Olson, D. M., Griffis, T. J., Noormets, A., Kolka, R., & Chen, J. (2013). Interannual, seasonal, and retrospective analysis of the methane and carbon dioxide budgets of a temperate peatland: Methane and carbon dioxide budgets. *Journal of Geophysical Research: Biogeosciences*, *118*(1), 226–238. <https://doi.org/10.1002/jgrg.20031>
- Pedersen, E. P., Michelsen, A., & Elberling, B. (2018). In situ CH₄ oxidation inhibition and ¹³CH₄ labeling reveal methane oxidation and emission patterns in a subarctic heath ecosystem. *Biogeochemistry*, *138*(2), 197–213. <https://doi.org/10.1007/s10533-018-0441-2>
- Pedregosa F, Varoquaux G, Gramfort A, Michel V, Thirion B, Grisel O, ... Duchesnay E. (2011). Scikit-learn: machine learning in Python. *Journal of Machine Learning Research*, *12*, 2825–30.
- Perryman, C. R., McCalley, C. K., Malhotra, A., Fahnestock, M. F., Kashi, N. N., Bryce, J. G., Giesler, R., & Varner, R. K. (2020). Thaw Transitions and Redox Conditions Drive Methane Oxidation in a Permafrost Peatland. *Journal of Geophysical Research: Biogeosciences*, *125*(3). <https://doi.org/10.1029/2019JG005526>
- Popp, T. J., Chanton, J. P., Whiting, G. J., & Grant, N. (2000). Evaluation of methane oxidation in the rhizosphere of a *Carex* dominated fen in north central Alberta, Canada. *Biogeochemistry*, *51*, 259–281.
- Quast, C., Pruesse, E., Yilmaz, P., Gerken, J., Schweer, T., Yarza, P., ... Glöckner, F. O. (2013). The SILVA ribosomal RNA gene database project: Improved data processing and web-based tools. *Nucleic Acids Research*, *41*(D1), 590–596. <https://doi.org/10.1093/nar/gks1219>
- Rey-Sanchez, C., Bohrer, G., Slater, J., Li, Y.-F., Grau-Andrés, R., Hao, Y., Rich, V. I., & Davies, G. M. (2019). The ratio of methanogens to methanotrophs and water-level dynamics drive methane transfer velocity in a temperate kettle-hole peat bog. *Biogeosciences*, *16*(16), 3207–3231. <https://doi.org/10.5194/bg-16-3207-2019>
- Robroek, B. J. M., Jasse, V. E. J., Kox, M. A. R., Berendsen, R. L., Mills, R. T. E., Cécillon, L., Puissant, J., Meima-Franke, M., Bakker, P. A. H. M., & Bodelier, P. L. E. (2015). Peatland vascular plant functional types affect methane dynamics by altering microbial community structure. *Journal of Ecology*, *103*(4), 925–934. <https://doi.org/10.1111/1365-2745.12413>
- Rupp, D., Kane, E.S., Dieleman, C., Keller, J.K., & Turetsky, M. (2019). Plant functional group effects on peat carbon cycling in a boreal rich fen. *Biogeochemistry*, *144*, 305–327. <https://doi.org/10.1007/s10533-019-00590-5>
- Saarnio, S., Alm, J., Silvola, J., Lohila, A., Nykänen, H., & Martikainen, P. J. (1997). Seasonal variation in CH₄ emissions and production and oxidation potentials at microsites on an oligotrophic pine fen. *Oecologia*, *110*(3), 414–422. <https://doi.org/10.1007/s004420050176>
- Shoemaker, J. K., Varner, R. K., & Schrag, D. P. (2012). Characterization of subsurface methane production and release over 3 years at a New Hampshire wetland. *Geochimica et Cosmochimica Acta*, *91*, 120–139. <https://doi.org/10.1016/j.gca.2012.05.029>
- Siljanen, H. M. P., Saari, A., Krause, S., Lensu, A., Abell, G. C. J., Bodrossy, L., Bodelier, P. L. E., & Martikainen, P. J. (2011). Hydrology is reflected in the functioning and community composition of methanotrophs in the littoral wetland of a boreal lake: Spatial aspects of methanotrophs in littoral wetland. *FEMS Microbiology Ecology*, *75*(3), 430–445. <https://doi.org/10.1111/j.1574-6941.2010.01015.x>

- Smith, G. J., & Wrighton, K. C. (2019). Metagenomic Approaches Unearth Methanotroph Phylogenetic and Metabolic Diversity. *Current Issues in Molecular Biology*, 57–84. <https://doi.org/10.21775/cimb.033.057>
- Strom, L., Mastepanov, M., and Christensen, T. R. (2005). Species-specific effects of vascular plants on carbon turnover and methane emissions from wetlands. *Biogeochemistry*, 75(1), 65–82. <https://doi.org/10.1007/s>
- Sundh, I., Nilsson, M., Granberg, G., & Svensson, B. H. (1994). Depth distribution of microbial fgreenproduction and oxidation of methane in northern boreal peatlands. *Microbial Ecology*, 27(3). <https://doi.org/10.1007/BF00182409>
- Sundh, I., Mikkela, C., Nilsson, M., & Svensson, B. H. (1995). Potential aerobic methane oxidation in a sphagnum- dominated peatland—Controlling factors and relation to methane emission. *Soil Biology and Biochemistry*, 27(6), 829–837. [http://doi.org/10.1016/0038-0717\(94\)00222-M](http://doi.org/10.1016/0038-0717(94)00222-M)
- Treat, C. C., Bubier, J. L., Varner, R. K., & Crill, P. M. (2007). Timescale dependence of environmental and plant-mediated controls on CH₄ flux in a temperate fen. *Journal of Geophysical Research*, 112(G1), G01014. <https://doi.org/10.1029/2006JG000210>
- Tremblay, J., Singh, K., Fern, A., Kirton, E. S., He, S. M., Woyke, T., ... Tringe, S. G. (2015). Primer and platform effects on 16S rRNA tag sequencing. *Frontiers in Microbiology*, 6, 771. doi: 10.3389 /fmicb.2015.00771
- Urbanová, Z., & Bárta, J. (2020). Recovery of methanogenic community and its activity in long-term drained peatlands after rewetting. *Ecological Engineering*, 150. <https://doi.org/10.1016/j.ecoleng.2020.105852>
- van Winden, J. F., Reichart, G.-J., McNamara, N. P., Benthien, A., & Damsté, J. S. Sinninghe. (2012). Temperature-Induced Increase in Methane Release from Peat Bogs: A Mesocosm Experiment. *PLoS ONE*, 7(6), e39614. <https://doi.org/10.1371/journal.pone.0039614>
- Vanwonterghem, I., Evans, P., Parks, D. et al. (2016). Methylotrophic methanogenesis discovered in the archaeal phylum Verstraetearchaeota. *Nature Microbiology*, 1, 16170. <https://doi.org/10.1038/nmicrobiol.2016.170>
- Waddington, J. M., Roulet, N. T., & Swanson, R. V. (1996). Water table control of CH₄ emission enhancement by vascular plants in boreal peatlands. *Journal of Geophysical Research: Atmospheres*, 101(D17), 22775–22785. <https://doi.org/10.1029/96JD02014>
- Wang, M., Tian, J., Bu, Z., Lamit, L.J., Chen, H., Zhu, Q., & Peng, C. (2019). Structural and functional differentiation of the microbial community in the surface and subsurface peat of two minerotrophic fens in China. *Plant and Soil*, 437, 21-40. <https://doi.org/10.1007/s11104-019-03962-w>
- Wetzel, R. G. (2001). Iron, Sulfur, and Silica Cycles. In *Limnology* (pp. 289–330). Elsevier. <https://doi.org/10.1016/B978-0-08-057439-4.50018-6>
- Whalen, Stephen C., Reeburgh, William S., & Barber, Valerie, A. (1992). Oxidation of methane in boreal forest soils: A comparison of seven measures. *Biogeochemistry*, 16(3). <https://doi.org/10.1007/BF00002818>
- Whiticar, Michael J. (1999). Carbon and hydrogen isotope systematics of bacterial formation and oxidation of methane. *Chemical Geology*, 161(1–3), 291–314. [https://doi.org/10.1016/S0009-2541\(99\)00092-3](https://doi.org/10.1016/S0009-2541(99)00092-3)
- Whiticar, M.J, Faber, E., & Schoell, M. (1986). Biogenic methane formation in marine and freshwater environments: CO₂ reduction vs. acetate fermentation—Isotope evidence.

Geochimica et Cosmochimica Acta, 50(5), 693–709. [https://doi.org/10.1016/0016-7037\(86\)90346-7](https://doi.org/10.1016/0016-7037(86)90346-7)

- Wickham, H. ggplot2: Elegant Graphics for Data Analysis. Springer-Verlag New York, 2016.
- Yrjälä, K., Tuomivirta, T., Juottonen, H., Putkinen, A., Lappi, K., Tuittila, E.-S., Penttilä, T., Minkkinen, K., Laine, J., Peltoniemi, K., & Fritze, H. (2011). CH₄ production and oxidation processes in a boreal fen ecosystem after long-term water table drawdown: CH₄ production and oxidation processes. *Global Change Biology*, 17(3), 1311–1320. <https://doi.org/10.1111/j.1365-2486.2010.02290.x>
- Yu, Z. C. (2012). Northern peatland carbon stocks and dynamics: A review. *Biogeosciences*, 9(10), 4071–4085. <https://doi.org/10.5194/bg-9-4071-2012>
- Zalman, C., Keller, J. K., Tfaily, M., Kolton, M., Pfeifer-Meister, L., Wilson, R. M., Lin, X., Chanton, J., Kostka, J. E., Gill, A., Finzi, A., Hoppo, A. M., Bohannon, B. J. M., & Bridgham, S. D. (2018). Small differences in ombrotrophy control regional-scale variation in methane cycling among Sphagnum-dominated peatlands. *Biogeochemistry*, 139(2), 155–177. <https://doi.org/10.1007/s10533-018-0460-z>

Table 1. Description of environmental conditions in the hummock and lawn sample plots. Values are reported as mean \pm standard deviation. Water table depth indicates the distance of the water table below the peat surface.

Microform	Dominant vascular vegetation	Water Table Depth (cm) ^a	Depth (cm)	pH ^b	Redox potential (Eh) ^b
Hummock (n = 4)	<i>Vaccinium oxycoccos</i> , <i>Chamaedaphne calyculata</i> , <i>Acer rubrum</i>	13.5 \pm 1.9 (24.5 \pm 1.5)	10	4.14 \pm 0.13	124.6 \pm 13.2
			30	4.34 \pm 0.12	115.7 \pm 18.3
			60	4.98 \pm 0.24	107.9 \pm 25.2
Lawn (n = 4)	<i>Vaccinium oxycoccos</i> , <i>Chamaedaphne calyculata</i> , <i>Carex rostrata</i>	8.5 \pm 3.1 (12.5 \pm 0.5)	10	4.23 \pm 0.24	117.2 \pm 21.4
			30	4.30 \pm 0.15	108.3 \pm 17.2
			60	4.57 \pm 0.19	81.1 \pm 23.8

^aTop value measured at time of microbial sampling in 2014, value in parentheses reports mean water table depth measured at wells central to the hummock and lawn plots during 2020 porewater sampling. ^bMeasured during porewater sampling in 2020.

Figure. 1 Depth profiles of potential CH₄ production rates (A) and potential CH₄ oxidation rates (B) in the lawn (green symbols) and hummock cores (orange symbols) extracted in 2018 from Sallie's Fen. Points represent the mean observed value, error bars indicate the standard deviation of the mean of 3 technical replicates from each core. Panel C displays dissolved oxygen measurements collected at the two plots cored for incubations in 2018. For all panels, horizontal lines represent the water table depth in each plot at the time of coring and dissolved oxygen measurements.

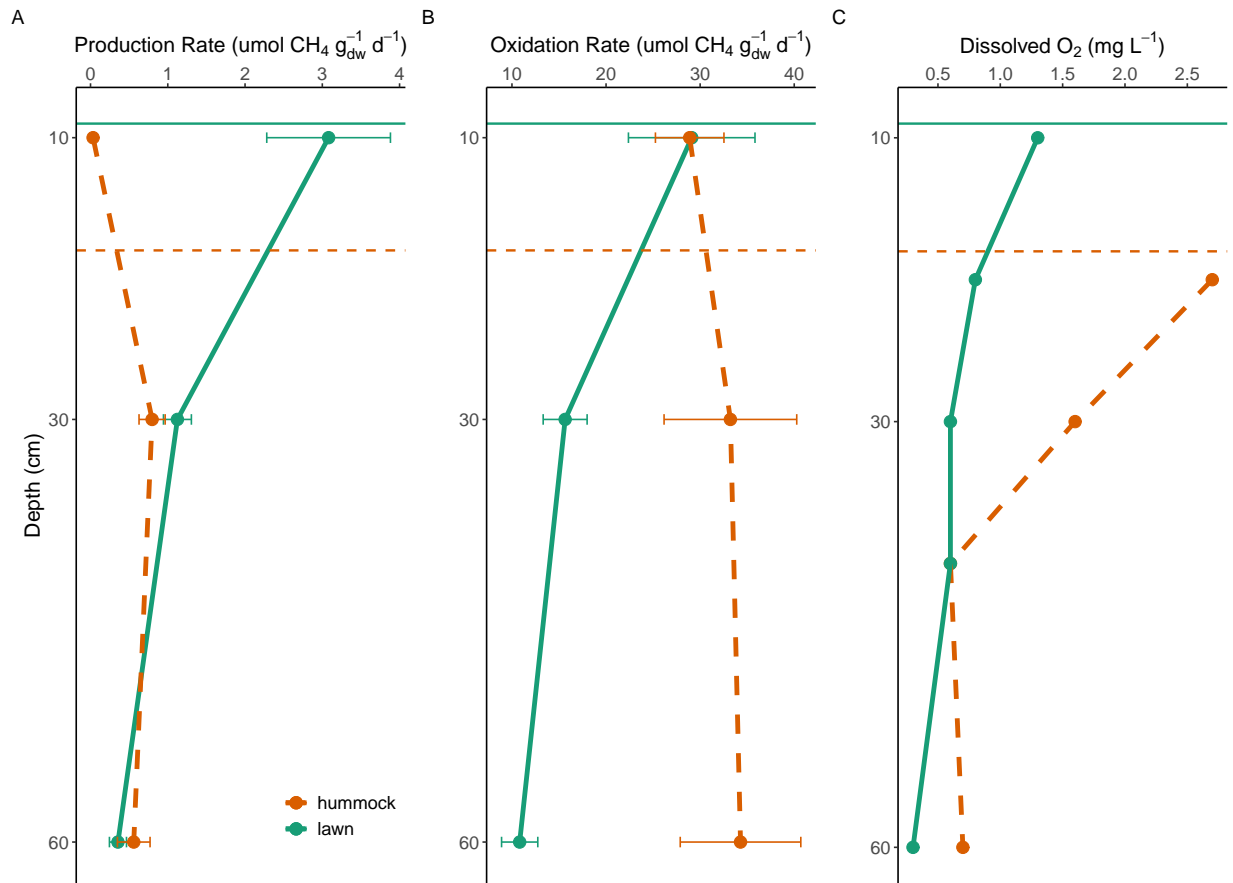
Figure. 2 Depth profiles of (A) dissolved CH₄, (B) porewater $\delta^{13}\text{C-CH}_4$, and (C) porewater $\delta\text{D-CH}_3\text{D}$ from lawns (green symbols) and hummocks (orange symbols) sites at Sallie's Fen, in Barrington, NH. Points represent the mean observed value, error bars indicate the standard deviation of the mean

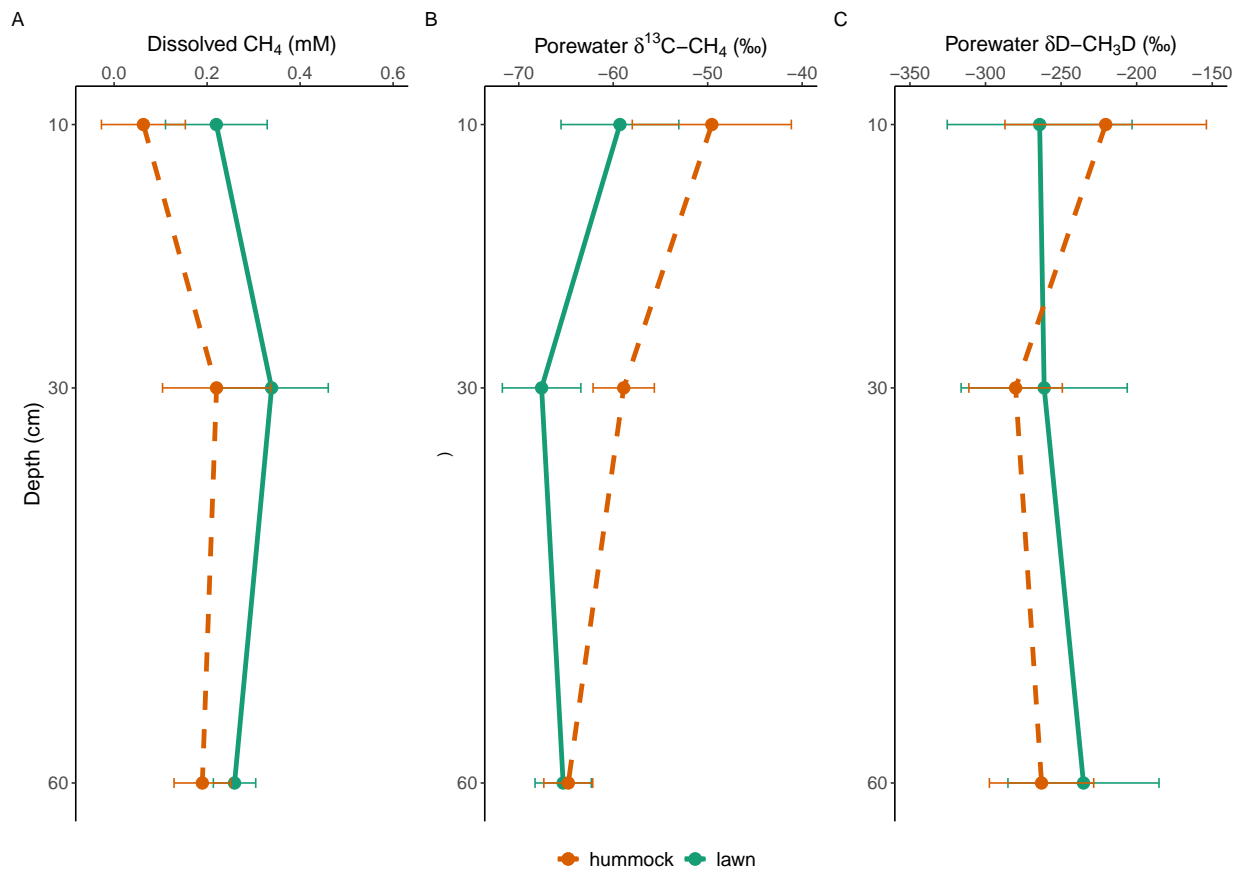
Figure. 3 Relationship between peat porewater $\delta^{13}\text{C-CH}_4$ and $\delta\text{D-CH}_3\text{D}$ from lawns (green symbols) and hummocks (orange symbols) at Sallie's Fen, Barrington, NH collected July-August 2020. Squares, circles, and triangles represent measurements from 10 cm, 30 cm, and 60 cm, respectively. (A) Average $\delta^{13}\text{C-CH}_4$ and $\delta\text{D-CH}_3\text{D}$ values at each depth in the lawns and hummocks. Each point represents the mean isotopic value from the 3 sample collections, error bars represent ± 1 standard deviation of the mean. (B) Individual measurements of porewater $\delta^{13}\text{C-CH}_4$ and dissolved CH₄ from the 3 sample collections (n = 54, R²_m = 0.30, F_{1,49} = 26.2, p < 0.001).

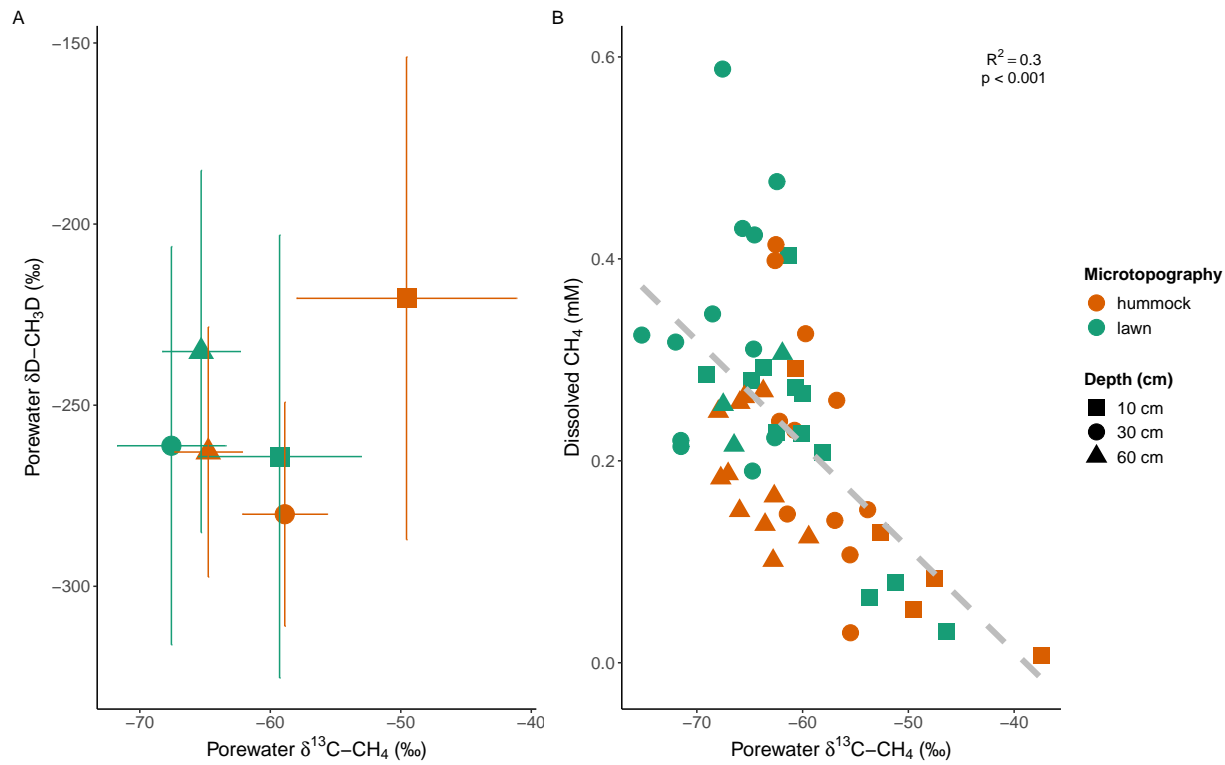
Figure. 4 (A) Depth profile of the ratio of the relative abundance of methanotrophs to methanogens from lawns (green symbols) and hummocks (orange symbols) sites at Sallie's Fen, in Barrington, NH. Points represent the mean observed value, error bars indicate the standard deviation of the mean. (B) NMDS plot of Bray-Curtis distance between samples collected from lawns (green symbols) and hummocks (orange symbols) for methanogenic and methanotrophic lineages (stress = 0.07). Squares, circles, and triangles represent measurements from 10 cm, 30

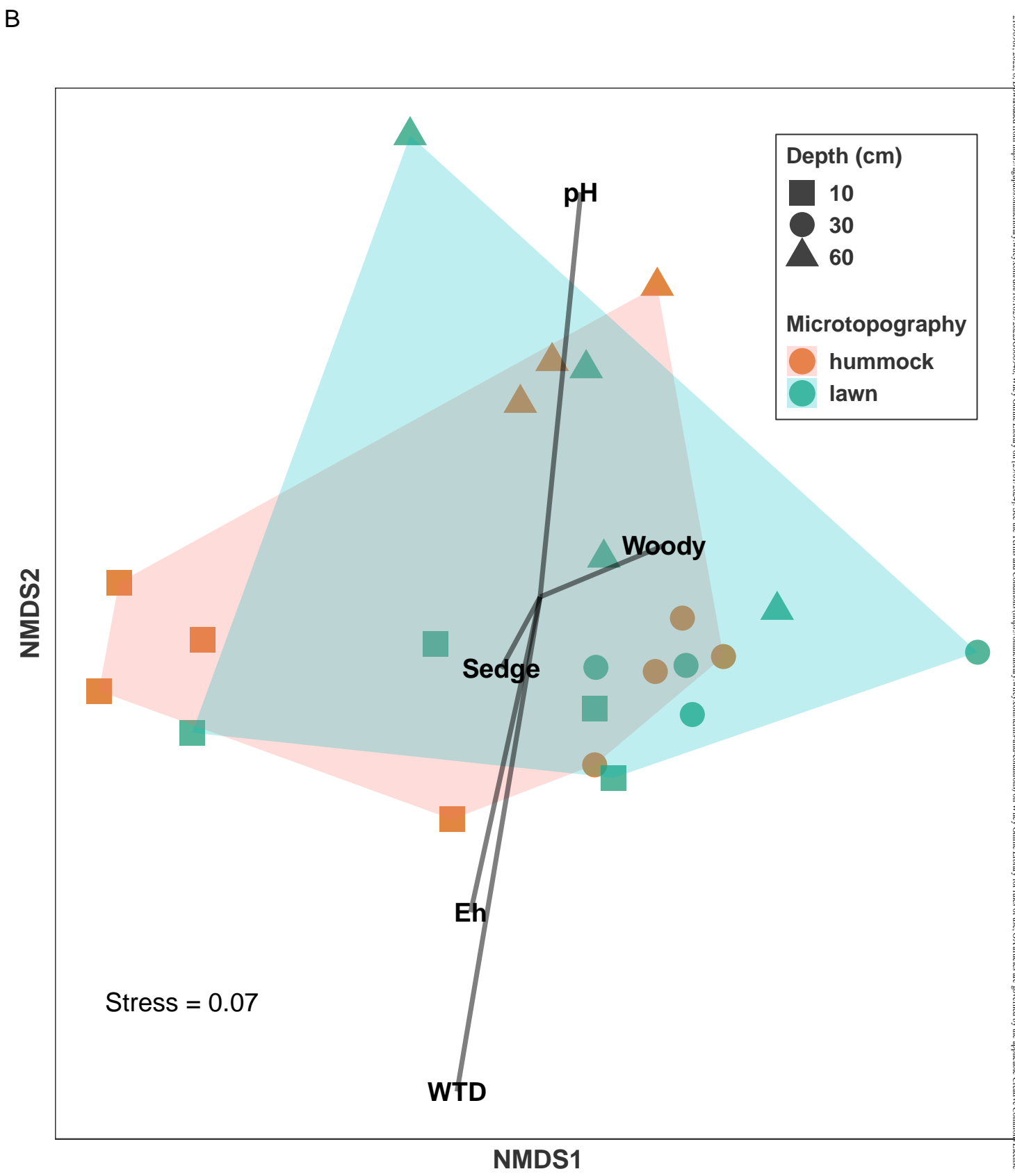
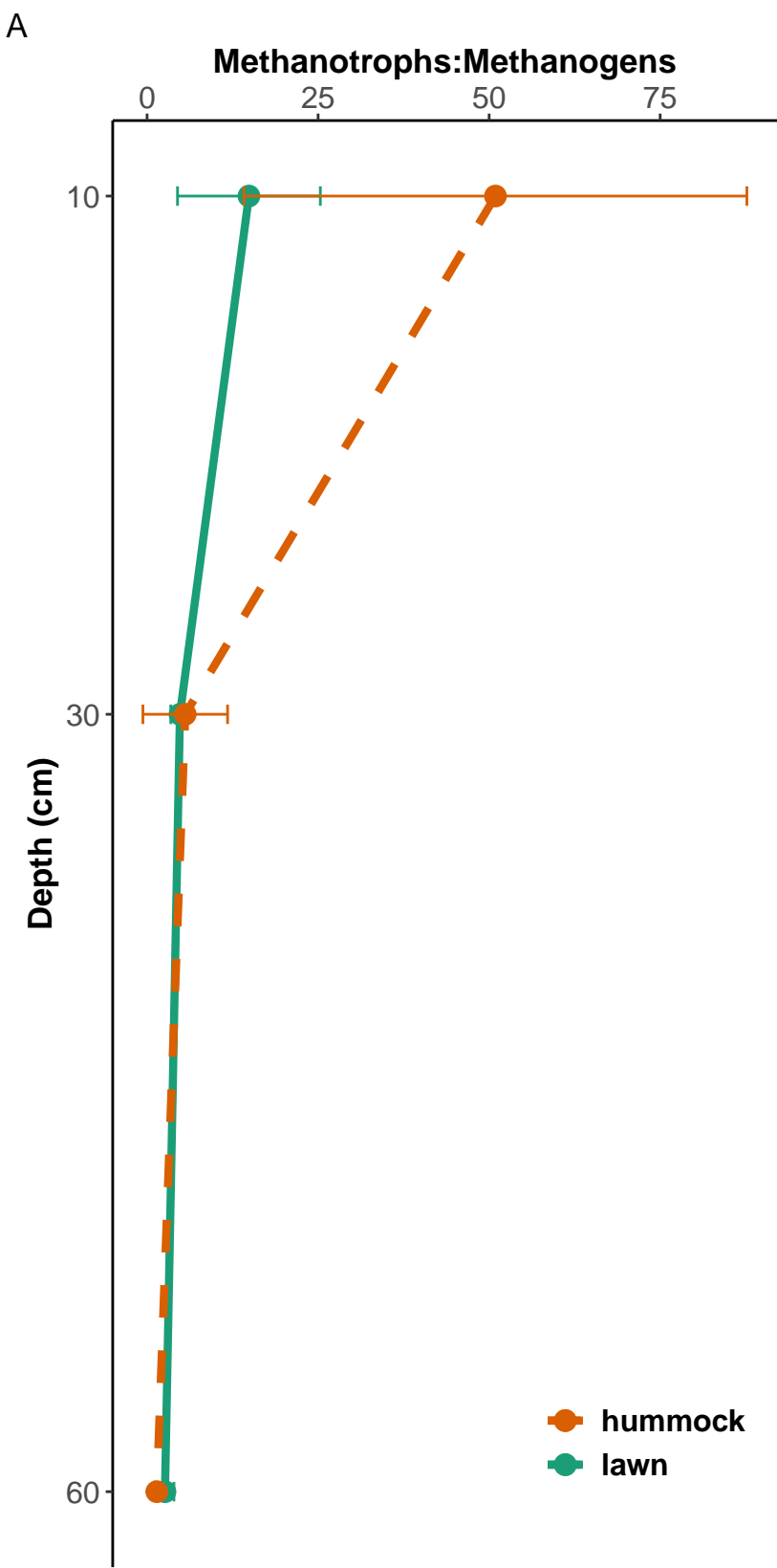
cm, and 60 cm, respectively. Community composition of methanogenic and methanotrophic taxa varied strongly between sample depths (PERMANOVA, $F = 8.33$, $R^2 = 0.44$, $p = 0.002$). Biplot vectors fit using `envfit()` reflect the directions in which environmental measurements correlate most strongly with the ordination configuration, with longer lines representing stronger correlations. For environmental vectors: Eh = redox potential, WTD = distance below the water table, Sedge = percent cover of *C. rostrata*, and Woody = percent cover of shrubs and deciduous trees

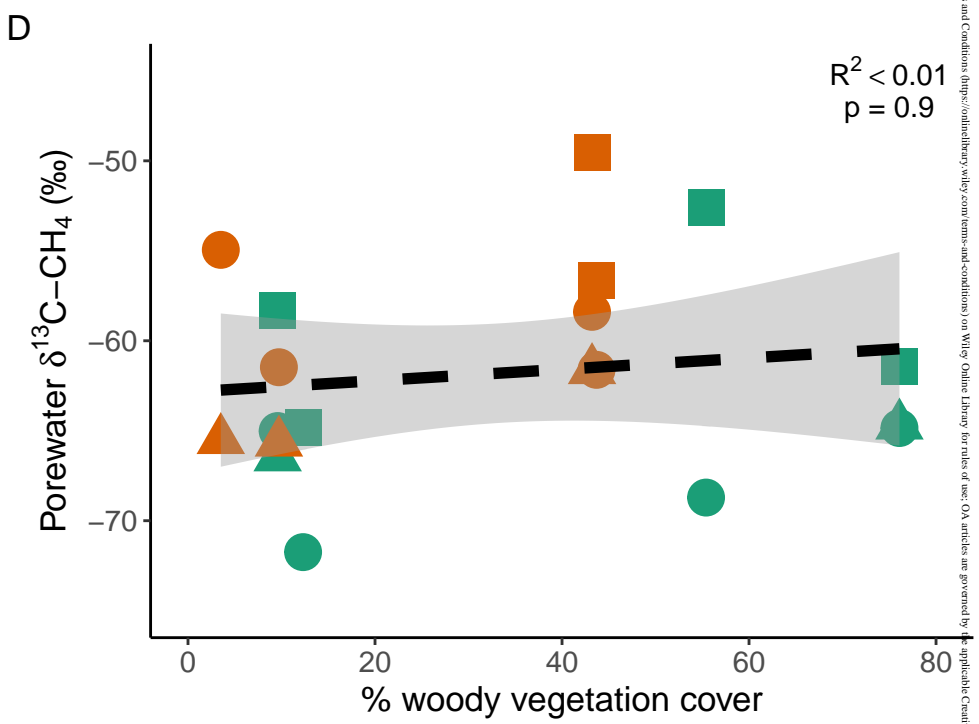
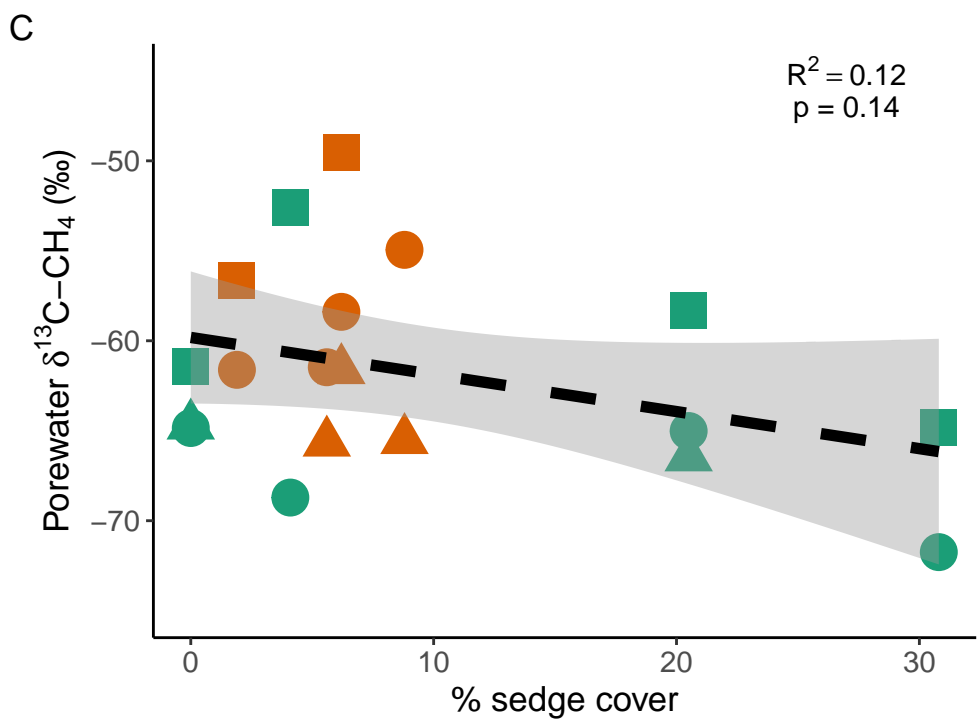
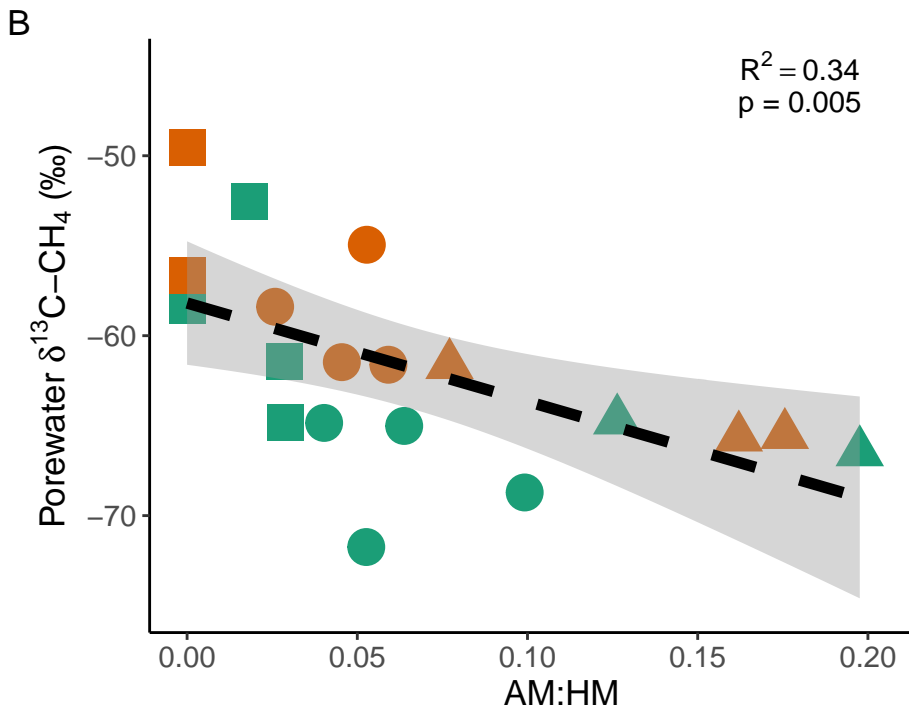
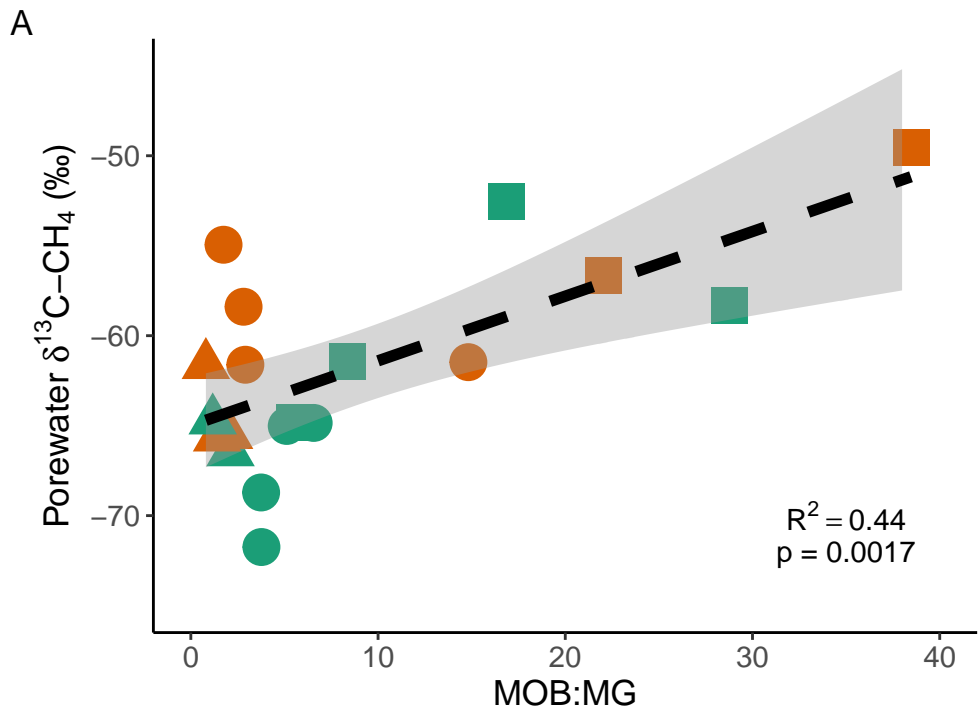
Figure. 5 Scatter plots of porewater $\delta^{13}\text{C}\text{-CH}_4$ and the (A) ratio of the relative abundance of methanotrophs to methanogens; MOB:MG, (B) ratio of the relative abundance of acetoclastic methanogens to hydrogenotrophic methanogens; AM:HM, (C) percent of sedge cover in the corresponding sample plot, and (D) percent of woody vegetation cover in the corresponding sample plot. R^2 and p values represent the results of LME. Plotted porewater $\delta^{13}\text{C}\text{-CH}_4$ represent the mean value observed over the 3 sample collections. Green points represent lawns and orange plots represent hummocks. Squares, circles, and triangles represent measurements from 10 cm, 30 cm, and 60 cm, respectively











■ 10 cm ● 30 cm ▲ 60 cm ● hummock ● lawn